A record of assimilation preserved by exotic minerals in the lowermost platinum-group element deposit of the Bushveld Complex: The Volspruit Sulphide Zone

Dominique Tanner [a,b,*], Iain McDonald [b], R.E. Jock Harmer [c], Duncan D. Muir [b], Hannah S.R. Hughes [d,e]

[a] GeoQuEST Research Centre, School of Earth and Environmental Sciences, University of Wollongong, NSW 2522, Australia
[b] School of Earth & Ocean Sciences, Cardiff University, Main Building, Park Place, Cardiff CF10 3AT, United Kingdom
[c] Department of Geology, Rhodes University, P.O. Box 94, Grahamstown 6140, South Africa
[d] Camborne School of Mines, College of Engineering, Mathematics and Physical Sciences, University of Exeter, Penryn Campus, Penryn TR10 9FE, United Kingdom
[e] School of Geosciences, University of the Witwatersrand, Private Bag 3, Wits, 2050, South Africa

ABSTRACT

Low-grade platinum-group element mineralisation in the Volspruit Sulphide Zone is sulphide-poor (<5 vol. %), distributed over a ~60 m-thick horizon in the lowermost cumulates of the northern limb of the Bushveld Complex. Unlike any other platinum-group element (PGE) deposit of the Bushveld Complex, the Volspruit Sulphide Zone is hosted exclusively within harzburgitic and dunitic cumulates in the Lower Zone of the Rustenburg Layered Suite.

Here, we present a petrological investigation on the distribution of PGEs and chalcophile metals in mineralised pyroxenite cumulates from the Volspruit Sulphide Zone, to determine the origin of the PGE mineralisation in ultramafic cumulates and evaluate whether Volspruit-style mineralisation could occur in the stratigraphically lowest, ultramafic portions of other layered intrusions.

Electron microscopy of pyroxenite cumulates revealed (1) chromite inclusions containing dolomite, albite, monazite, Pb-chlorides, base metal sulphides and Pt-As minerals, (2) the presence of exotic microxenocrysts (<300 μm diameter) in the pyroxenite matrix such as grains of $CaCO_3$, U-Th-oxide and Mn-ilmenite, and (3) base metal sulphide assemblages enclosing grains of primary galena, sphalerite and Pb-chlorides.

Systematic mapping of high-density mineral assemblages in pyroxenite cumulates across the Volspruit Sulphide Zone identified 196 precious metal mineral grains (Pt-, Pd-, Rh-, Au- or Ag-minerals), 98 Pb-sulphide grains (± Se, Cl), 27 Pb-chloride grains (± K, Se, Te, S), as well as 1 grain of Pb-telluride, 1 monazite grain and 1 grain of U–Pb-Th oxide. Trace element analyses of base metal sulphides reveal the highest S/Se values in pyrrhotite and chalcopyrite yet recorded in the Bushveld Complex. While some base metal sulphides are enriched in PGEs, the overall low-grade of the deposit and inferred fertile ultramafic magma(s) require relatively low R-factors (mass of silicate to sulphide melt) compared to other sulphide-poor PGE deposits, with a calculated R factor of ~500–3000. We consider that the presence of exotic inclusions in chromite, exotic microxenocrysts, and Pb/Zn/Cl grains enclosed within primary base metal sulphide assemblages provide strong evidence for crustal contamination in the Volspruit Sulphide Zone. The Malmani dolomite and the Black Reef quartzite within the lower Chuniespoort Group (2.2–2.4 Ga) are the most likely source of xenocrysts, assimilated in a staging chamber beneath the main Grasvally chamber, in which the Volspruit Sulphide Zone developed. It is possible that the Malmani dolomite contained an enrichment of Pb, Zn, Cl, and S minerals prior to assimilation. The assimilation of dolomite and limestone would locally increase the fO_2 of the magma, triggering chromite crystallisation. The sudden removal of Fe from the melt, coupled with the addition of external sulfur triggered saturation of an immiscible sulphide melt in the ultramafic Volspruit magma. Chromite and base metal sulphides were subsequently emplaced into the main Grasvally magma chamber as a crystal-bearing slurry. Therefore, we consider it is possible for PGE mineralisation to occur in the ultramafic portion of any layered intrusion intruding in the vicinity of carbonate units. Even if this style of mineralisation in the lowermost portions of layered intrusions is subeconomic, it may reduce the grade or opportunity for PGE mineralisation higher up in the local magmatic stratigraphy, or in later magma emplacement events sourced from the same reservoir.

* Corresponding author at: GeoQuEST Research Centre, School of Earth and Environmental Sciences, University of Wollongong, NSW 2522, Australia
E-mail address: dtanner@uow.edu.au (D. Tanner).

The technique of specifically searching for microxenocrysts could be applied beyond layered intrusion research, to identify the range of crustal contaminants in other magmatic systems where macro-scale xenoliths are neither sampled nor preserved.

1. Introduction

Platinum-group element (PGE) mineralisation in layered intrusions typically occurs as stratiform reefs in the lower to central portions of an intrusive body, following some degree of magmatic differentiation (e.g. Maier, 2005; Naldrett, 2004). Stratiform PGE deposits hosted exclusively in the lowermost, least evolved peridotitic or pyroxenitic portions[1] of a layered intrusion are relatively uncommon (Maier, 2005). Here, we investigate the distribution of precious metals and chalcophile elements in the Volspruit Sulphide Zone – the lowermost and least evolved PGE deposit of the Bushveld Complex – hosted entirely within pyroxenite. These results will be used to: (1) identify ore-forming processes that concentrate PGEs exclusively within ultramafic cumulates, and (2) evaluate whether Volspruit-style PGE mineralisation could occur elsewhere in the Bushveld Complex, or in less-explored layered intrusions.

1.1. Geological setting

The Bushveld Complex comprises three suites of plutonic rocks: (1) the Rustenburg Layered Suite (layered ultramafic to mafic cumulates), crosscut by (2)the Rashoop Granophyre Suite and (3)the Lebowa Granite Suite (von Gruenewaldt and Walraven, 1980). The focus of this study is the mineralised Volspruit Sulphide Zone in the Lower Zone of the ca. 2056 Ma Rustenburg Layered Suite, the largest known layered mafic intrusion on Earth (Cawthorn, 2015; Zeh et al., 2015). The Rustenburg Layered Suite is divided into five lobe-shaped limbs (Fig. 1a) which span an area of >40,000 km^2 (Cawthorn, 2015). Recently, a northern extension of the Rustenburg Layered Suite has been described at the Waterberg project (Huthmann et al., 2018; Kinnaird et al., 2017).

The Rustenburg Layered Suite comprises a series of layered cumulate horizons ≤7 km thick (Cawthorn, 2015) (Fig. 2), subdivided into five informal subzones[2]: the noritic Marginal Zone, the ultramafic Lower Zone, the mafic-ultramafic, chromite-bearing Critical Zone, the mafic Main Zone and the mafic, magnetite-bearing Upper Zone. Recently, additional informal subzones have been defined: the Basal Ultramafic Sequence in the eastern limb (Wilson, 2015) and subzones within the Waterberg project (Kinnaird et al., 2017). The stratigraphic correlation of the northern limb is summarised in Fig. 2, including our interpretation of the relationship between the Lower Zone of the northern limb and the recently-defined stratigraphic subzones of the Rustenburg Layered Suite. While known PGE mineralisation in the eastern and western limbs is confined to the Critical Zone, the northern limb contains PGE mineralisation at a range of stratigraphic intervals (Figs. 2 and 3).

1.1.1. The Lower Zone of the Rustenburg Layered Suite
Formally, the Lower Zone in the eastern and western limbs of the Bushveld Complex comprises the Croydon Subsuite and the Vlakfontein Subsuite, respectively. The top of these subsuites is defined by the absence of cumulus chromite (South African Committee for Stratigraphy, 1980). However the Lower Zone of the northern limb, the Zoetveld Subsuite, contains cumulus chromite and multiple chromitite seams (van der Merwe, 2008).

Informally, the Lower Zone in the eastern and western limbs of the Bushveld Complex is defined by either the increase from ≤2% to ≥ 6% vol. % intercumulus plagioclase (Cameron, 1978), or the top of the olivine-rich interval ~200 m above the increase to ≥ 6% vol. % intercumulus plagioclase (Teigler and Eales, 1996).

The mineralised Volspruit Sulphide Zone is hosted within the Volspruit subzone, in the Lower Zone of the northern limb (Fig. 2). Fig. 3 demonstrates that there is ≤2 vol. % plagioclase throughout the Volspruit subzone, including the interval of the Volspruit Sulphide Zone. While accessory chromite is present (Fig. 3), no chromitite seams occur within the Volspruit subzone (Hulbert, 1983). So despite the presence of cumulus chromite, we consider the Lower Zone of the northern limb cannot be analogous to the Lower Critical Zone in the eastern and western limbs of the Bushveld Complex.

As observed by van der Merwe (1976), mineral compositions in the Lower Zone of the northern limb (En$_{77}$-En$_{91}$; Fo$_{85}$-Fo$_{95}$; Hulbert, 1983; Wilson, 2015; Yudovskaya et al., 2013), contain greater Mg content than minerals from the Lower Zone of the eastern limb (En$_{67}$-En$_{88}$; Fo$_{84}$-Fo$_{87}$; Wilson, 2015; Yudovskaya et al., 2013) (Fig. 2). Based on the relatively unevolved mineral compositions, we propose that the Lower Zone of the northern limb is more akin to the Basal Ultramafic Sequence of the eastern limb (En$_{71}$-En$_{92}$; Fo$_{82}$-Fo$_{92}$; Wilson, 2015; Yudovskaya et al., 2013) than the Lower Zone of the eastern limb.

1.1.2. Platinum-group element (PGE) mineralisation in the Rustenberg Layered Suite
PGE deposits within layered ultramafic to mafic cumulate rocks of the Rustenburg Layered Suite host 70.9% of known global platinum resources (Mudd 2012). These PGE resources are hosted within the Critical Zone (in the eastern and western limbs), the Platreef (in the northern limb, north of Mokopane), or the Grasvally Norite-Pyroxenite-Anorthosite (GNPA) member (in the northern limb, south of Mokopane) within the Rustenburg Layered Suite. In 2014, 163 PGE resources[3] were defined in the Bushveld Complex (Zientek et al., 2014). Of these 163 resources, the Volspruit (Ni-PGE) Sulphide Zone is the only deposit known to occur in an exclusively ultramafic sequence (i.e. in cumulates where mafic minerals constitute >90% of the rock).

Ni-PGE mineralisation also occurs within the Ultramafic Sequence of the Waterberg project, an extension to the northern limb of the Bushveld Complex (Huthmann et al., 2018; Kinnaird et al., 2017). However, this Ultramafic Sequence is not ultramafic (c.f. Le Maître et al., 2002) as "the amount of interstitial plagioclase in the Waterberg ultramafic rocks commonly exceeds 10-15 vol. % …" (page 1383, Kinnaird et al., 2017). Similarly, PGE mineralisation is documented in Lower Zone lithologies beneath the Platreef at Turfspruit, in the northern limb of the Bushveld Complex (Yudovskaya et al., 2014, 2013), yet again, this mineralisation is not hosted exclusively within ultramafic lithologies. Where modal abundance data are presented for the drill core UMT006 at Turfspruit (Yudovskaya et al., 2014), it is evident that the only portions of the Lower Zone exhibiting elevated PGE concentrations

---

[1] By peridotitic and pyroxenitic, we specifically mean horizons containing <10 vol. % felsic minerals (e.g. plagioclase) and > 90% mafic minerals (e.g. olivine and/or pyroxene) viz. Le Bas and Streckeisen (1991); Le Maître et al. (2002); Streckeisen (1976).

[2] The (South African Committee for Stratigraphy, 1980) do not officially recognise these informal subzones and would prefer workers to refer to the names of local subsuites. For example, the term for the Lower Zone of the northern limb of the Bushveld Complex is the Zoetveld Subsuite. In this paper we have followed the precedent to use the names of informal subzones instead, to reduce confusion for readers.

[3] Resources explicitly defined by a national code for reporting the results of mineral exploration. Typically, Bushveld resources are defined according to the South African Code for the Reporting of Exploration Results, Mineral Resources And Mineral Reserves (SAMREC Code), or the Australasian Code for Reporting of Exploration Results, Mineral Resources and Ore Reserves (the JORC Code) – depending on which stock exchange the exploration company is listed.
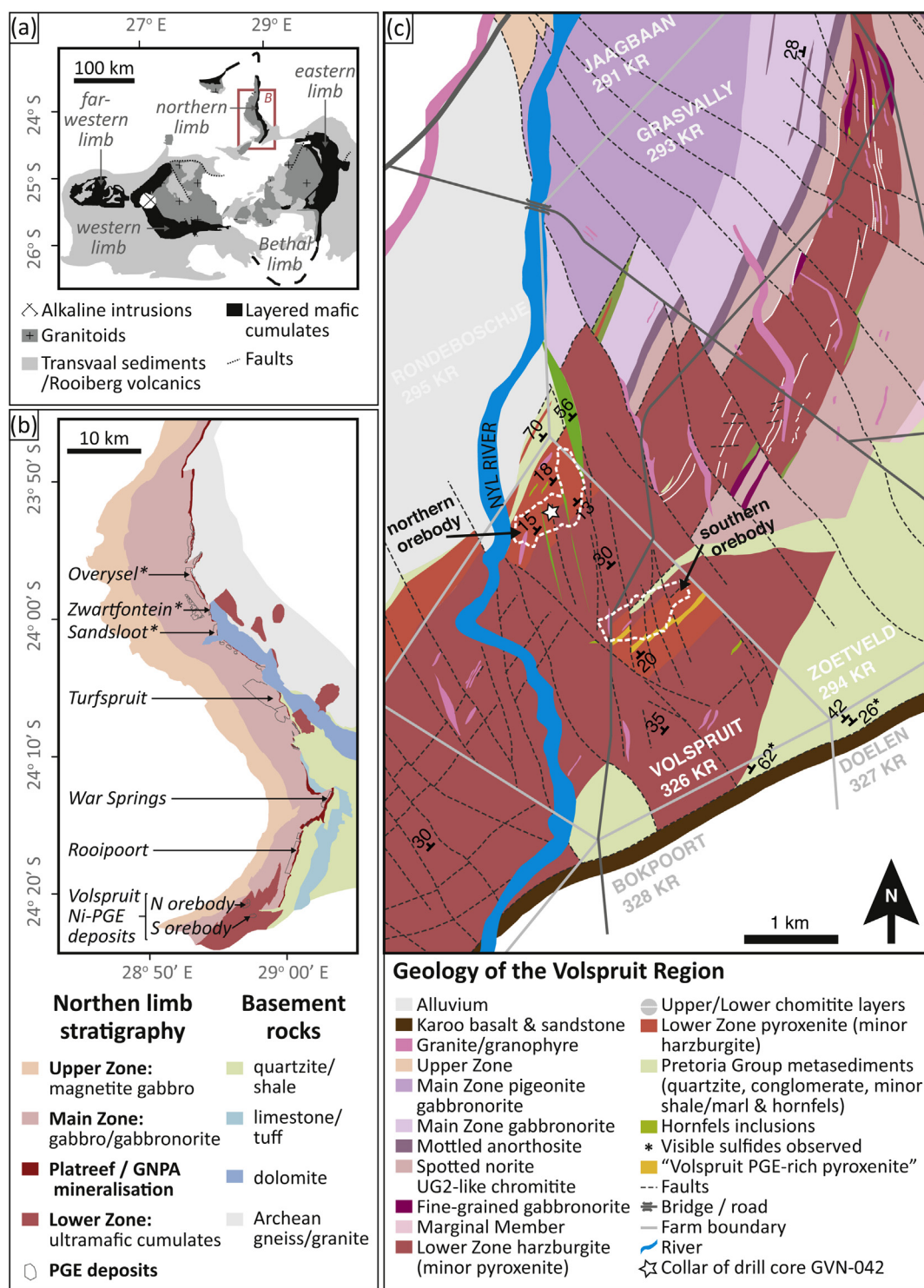
Fig. 1. Geological maps of the Bushveld Complex, northern limb, and Volspruit region. (a) Map showing the location of the five limbs of the Rustenburg Layered Suite. Map modified from Tanner et al. (2014). (b) Magmatic stratigraphy of the northern limb of the Rustenburg Layered Suite, highlighting the location of mineralisation in the Volspruit region in Lower Zone cumulates, compared to Platreef/GNPA mineralisation. Platreef/GNPA mineralisation occurs at the margin of the Rustenberg Layered Suite, between Main Zone cumulates and country rock. Map modified from Zientek et al. (2014). (c) Location of core GVN-042 (this study) is marked with a star. Proposed pit outlines of the northern and southern Volspruit Sulphide Zone orebodies are shown in white stippled lines (Pan Palladium Limited, 2008). Map modified from Hulbert (1983).

correspond with plagioclase pyroxenite, where plagioclase content exceeds 15 vol. %.

1.1.3. Spatially and temporally related Ni-PGE mineralisation in ultramafic lithologies

PGE mineralisation occurs in two ultramafic sequences (satellite intrusions) relatively proximal to and coeval with the Bushveld magmatic

event: the Nkomati Ni-Cu-Cr-PGE deposit in the Uitkomst Complex and subeconomic Ni-PGE concentrations within the Molopo Farms Complex (Kaavera et al., 2018; Maier et al., 2017; Prendergast, 2012). These localities are examples of sulphide-rich mineralisation as they contain intersections of massive sulphide: up to 99 vol. % massive sulphides at Nkomati and up to 30 vol. % net-textured sulphides at the Molopo Farms Complex (Prendergast, 2012; Theart and Nooy, 2001).
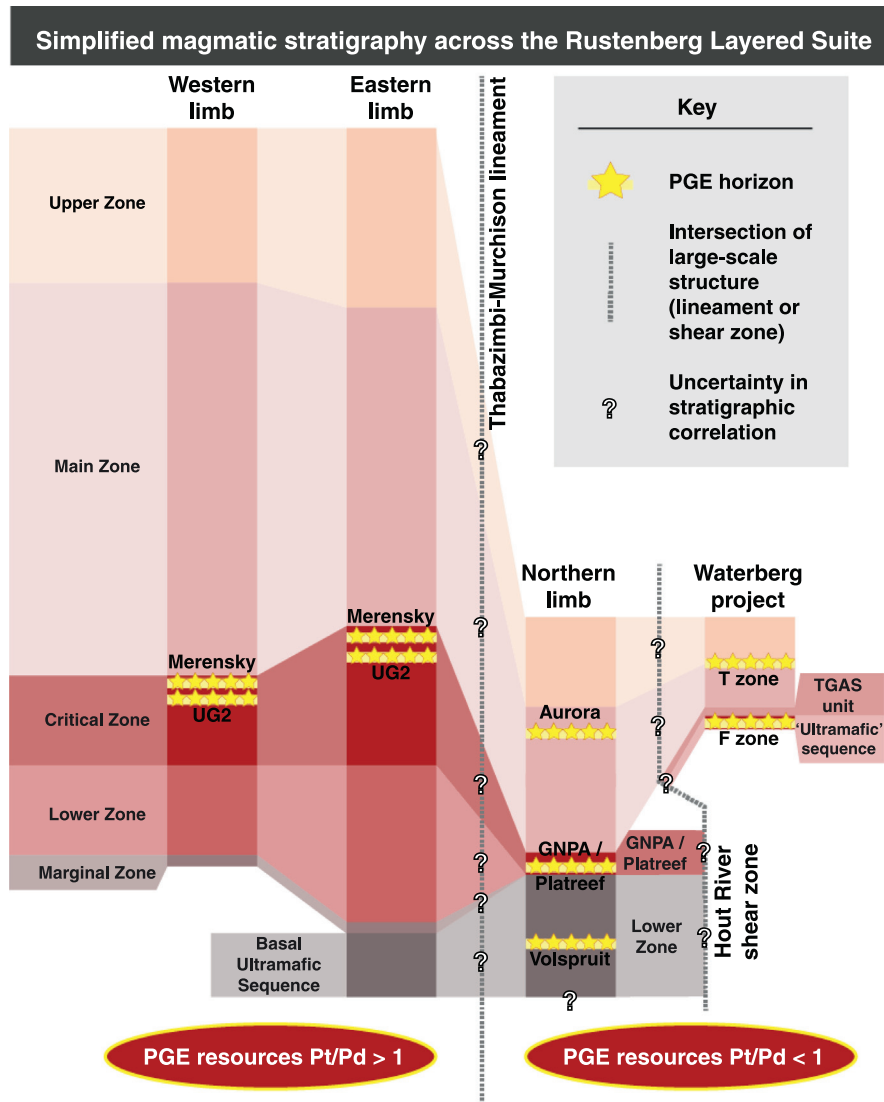
Fig. 2. Correlation of the simplified magmatic stratigraphy across the Rustenburg Layered Suite. Here, we propose that the Lower Zone of the northern limb is more akin to the Basal Ultramafic Sequence of the eastern limb than the Lower Zone of the eastern limb (refer to text for details). Mineralisation is shown by rows of yellow stars. This Fig. is schematic and not to scale, based on stratigraphic summaries of Joubert and Johnson (1998) and Kinnaird et al. (2017), with additional information from Eales and Cawthorn (1996), Kinnaird and McDonald (2005) and McDonald et al. (2016).

1.2. Geology of the Volspruit Sulphide Zone

The Volspruit Sulphide Zone[4] is a stratiform horizon enriched in Ni and PGEs (with an average grade of 0.14 wt% Ni and 1.25 ppm Pt + Pd + Au; Table 1), hosted within orthopyroxene-chromite cumulates of the Volspruit subzone in the Lower Zone of the northern limb (Fig. 3). The Volspruit Sulphide Zone constitutes the stratigraphically lowest occurrence of potentially economic PGE

mineralisation in the magmatic stratigraphy of the Rustenburg Layered Suite, and occurs in the least evolved cumulates of any Bushveld orebody (Fig. 2).

Petrologic field relationships in this region (Fig. 1c) were most comprehensively established by van der Merwe (1976, 2008) and Hulbert (1983). The Volspruit Sulphide Zone is located at least ~500 m above the base of the Rustenburg Layered Suite (Fig. 2 in Hulbert and von Gruenewaldt, 1982), however drill cores in the Volspruit region have not intersected the basement rocks beneath the Lower Zone (Hulbert, 1983; van der Merwe, 2008; Venmyn, 2010), so the depth of the Lower Zone remains unknown.

Two economic mineral resources are defined in the Volspruit Sulphide Zone: a northern and a southern orebody, both planned as open cut mines (the pit outlines of both orebodies are shown in Fig. 1b-c) (Sylvania Resources Ltd., 2010; Venmyn, 2010; Zientek et al., 2014). The northern orebody of the Volspruit Sulphide Zone (Fig. 1b-c) contains two-thirds of the defined resource. This orebody is described as a "flat lying" zone of PGE mineralisation with "an average vertical width of 59 m and strike length of approximately 1,800 m" (page 5, Venmyn, 2010), gently dipping ~15° to the NW (Hulbert, 1983). The

---

[4] We use the term "Volspruit Sulphide Zone" synonymously with the term "Volspruit Sulphide Layer" of Hulbert (1983). This zone of mineralisation is also sometimes referred to as "Cyclic Unit 11" of the Volspruit subzone (Hulbert and von Gruenewaldt, 1982), the "Volspruit Ni-PGE Reef" in technical mining reports (e.g. Venmyn, 2010), the "Grass Valley" project (e.g. Sylvania Resources Ltd., 2010), or "Grasvally" in academic literature (Maier et al., 2016; Yudovskaya et al., 2017). However, economic PGE mineralisation within the Volspruit Sulphide Zone has only been defined on the Volspruit and Zoetveld Farms, rather than the Grasvally Farm. This confusion is likely caused because the Lower Zone magma chamber in this region is often referred to as the "Grasvally chamber" or "Grasvally body" in academic literature (e.g. McDonald and Holwell, 2007; van der Merwe, 2008), so-called because economic chromitite seams of the Drummondlea subzone (Fig. 3) are mined at the Grasvally Chrome Mine on the Grasvally and Zoetveld Farms (Hulbert and von Gruenewaldt, 1985).
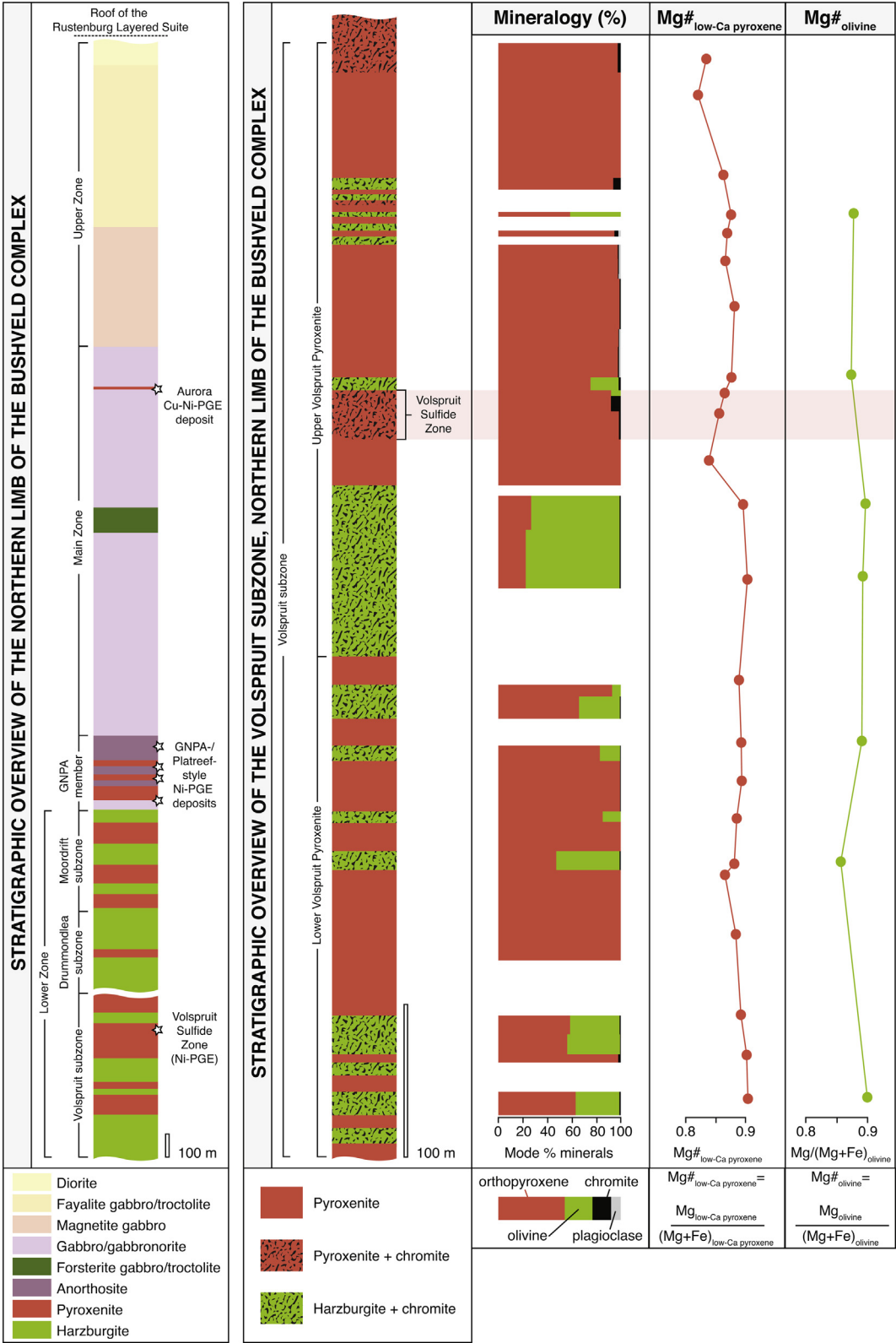
Fig. 3. Overview of the magmatic stratigraphy of the northern limb (left), and the Volspruit subzone, the lowermost portion of the Lower Zone in the northern limb (second from the left). Stratigraphic logs are modified from Hulbert (1983) with information from Kinnaird and McDonald (2005) and McDonald et al. (2016). Adjacent to the stratigraphic log, we present data on the mineralogy (modal percentage of minerals), the Mg# of orthopyroxene and the Mg# of olivine against stratigraphic depth in the Volspruit subzone, using data from Hulbert (1983). The interval containing mineralisation, the Volspruit Sulphide Zone, has been highlighted in pink shading to aid visual correlation between the three plots.

southern pit comprises the remainder of the resource: an orebody with an average vertical width of 47 m, dipping ~45° NW for 1 km along strike (Venmyn, 2010).

Faulting is evident in both orebodies, although detailed structural information is not available for this region (Venmyn, 2010). Based on the map of Hulbert (1983) (Fig. 1c), we suppose that the northern and

Table 1
Ore grades in the Volspruit Sulphide Zone, compared to other deposits in the northern limb of the Rustenburg Layered Suite.

Average grade and tonnage of PGE resources in the northern limb of the Bushveld Complex[a]

Ore deposit (from north to south)	Ni (wt%)	Cu (wt%)	Au (ppm)	Pt (ppm)	Pd (ppm)	Rh (ppm)	Mass of orebody (metric tons)	Ni/Cu	Pt/Pd
Aurora and Hacra Projects	0.03	0.05	0.00	0.48	0.78	0.00	123,495,000	0.69	0.61
Boikgantsho Project	0.11	0.08	0.07	0.77	0.74	0.00	128,252,000	1.41	1.03
Mogalakwena Mine	–	–	0.13	0.98	1.15	0.07	3,510,800,000		0.85
Akanani Project	0.18	0.10	0.15	1.08	1.43	0.09	130,100,000	1.80	0.75
Akanani Project	0.25	0.14	0.27	1.97	2.30	0.18	161,800,000	1.86	0.85
Turfspruit Project	0.15	0.13	0.05	0.39	0.46	–	776,400,000	1.19	0.85
Macalacaskop Project	0.17	0.11	0.07	0.51	0.60	–	251,000,000	1.55	0.85
Mokopane Project	0.15	0.09	0.00	0.22	0.33	–	39,700,000	1.72	0.67
War Springs Project	–	–	0.08	0.26	0.78	–	46,965,000		0.33
Rooipoort Project	0.19	0.11	0.09	0.47	0.72	–	18,128,000	1.73	0.66
Volspruit Project-North Pit[b]	0.14	0.04	0.02	0.56	0.67	–	50,933,000	3.62	0.83

Grade of samples from drillcore GVN-042, intersecting the Volspruit Sulphide Zone[c]

Sample	Depth range (m)	Ni (ppm)	Cu (ppm)	Au (ppb)	Pt (ppb)	Pd (ppb)	Rh (ppb)	Cr (ppm)	Sr (ppm)	Ni/Cu	Pt/Pd
7B	67.88–68.88	1514	340	60	1210	1535	220	14305	7	4.45	0.79
14A	87.88–88.88	2364	580	60	1065	1605	210	26816	12	4.08	0.66
16A, 16B	90.88–91.88	1709	361	70	1550	2090	270	18905	226	4.73	0.74
18B	96.88–97.88	2216	635	75	1440	1850	230	14673	11	3.49	0.78
22A, 22B	106.88–107.88	3595	1003	70	1310	1890	285	4576	8	3.58	0.69
25A	115.88–116.88	1808	497	55	2500	2255	225	18609	19	3.64	1.11
27B	120.88–121.88	2809	581	45	1200	1650	150	4401	13	4.83	0.73

[a] Data from Zientek et al. (2014).
[b] North Pit corresponds to the northern pit outline of the Volspruit Sulphide Zone shown in Fig. 1.
[c] Bulk assay data provided by Pan Palladium Ltd. (this study).

southern orebodies are the same Volspruit Sulphide Zone that have since experienced ~1.5 km of dextral displacement along a N-S striking fault.

Partially digested country rock xenoliths and associated partial melts of floor rocks are observed in a prominent ~100 m-thick harzburgite horizon that occurs a few tens of metres beneath the Volspruit Sulphide Zone; these features are less common in the pyroxenites of the Volspruit Sulphide Zone (EScience Associates (Pty) Ltd, 2011). Evidence of xenoliths and country rock assimilation is only briefly reported in one technical mining report; no evidence of these relationships is documented in peer-reviewed literature. To date, all published studies of the Volspruit Sulphide Zone have analysed pyroxenite samples (Hulbert, 1983; Hulbert and von Gruenewaldt, 1985, 1982; Paktunc et al., 1990; this study).

Preliminary studies suggest that Ni-PGE mineralisation is controlled by high-tenor (up to 195 ppm Pd and 11 ppm Ru in pentlandite), low-volume (2–3.6 vol. % sulphide) magmatic sulphide assemblages, with accessory platinum-group minerals (Hulbert, 1983; Hulbert and von Gruenewaldt, 1982; Paktunc et al., 1990). PGE mineralisation is hosted in relatively unfractionated orthopyroxenites (orthopyroxene chemistry = En$_{85}$-En$_{86}$) containing minor amounts of chromite (up to 47.52–46.61 wt% Cr_2O_3) (Hulbert, 1983) (Fig. 3). Bulk sulfur isotopes of the Volspruit Sulphide Zone are isotopically heavy ($\delta^{34}S = +3.8$ to $+4.3$ ‰) (data from Hulbert, 1983), relative to $\delta^{34}S$ values of the local mantle ($\delta^{34}S = -1.8$ to $+2.4$ ‰) derived from diamond-hosted sulphide inclusions in the Klipspringer kimberlite (Westerlund et al., 2004).

Hulbert and von Gruenewaldt (1982) document variable thickness of the Volspruit Sulphide Zone down dip – towards what they postulate as the centre of the intrusion. Hulbert and von Gruenewaldt (1982) state that the increase in thickness of the Volspruit Sulphide Zone is conincident with increasing grade of Pt, Pd and Cu, but only a marginal increase in the Ni grade. They attribute Ni-PGE mineralisation in the Volspruit Sulphide Zone to a combination of (1) gradually increasing sulfur in the magma via fractional crystallisation of ~500 m of ultramafic cumulates (i.e. the cyclic units beneath the Volspruit Sulphide Zone), with (2) an influx of a volumetrically small component of less primitive (i.e. basaltic) magma, that upon mixing with the resident magma,

created a decrease in temperature, resulting in sulfur saturation and chromite precipitation (Hulbert and von Gruenewaldt, 1982).

1.3. Sulphide-poorPGE mineralisation in the ultramafic portions of layered intrusions

Of 115 PGE deposits or occurrences in layered intrusions worldwide, Maier (2005) documented 18 PGE occurrences hosted within ultramafic silicate rocks from the lower portion of a layered intrusion. However, literature on cumulate rocks is fraught with petrologic inconsistencies caused by the range of proposed nomenclature schemes: the IUGS system (Le Bas and Streckeisen, 1991; Le Maître et al., 2002; Streckeisen, 1976), systems based on cumulus and intercumulus texture (Hunter, 1996; Irvine, 1980) and occasionally terms inherited from local mine geologists. In some cases, the lack of petrologic information makes it difficult to determine whether mineralisation was exclusively hosted within ultramafic cumulates (>90% mafic minerals), or in a mixture of mafic and ultramafic lithologies.

Magmatic sulphide deposits are divided into (1) Ni-Cu ore deposits with net-textured and/or massive sulphides (typically 20–90 vol. % sulphide; c.f. Naldrett, 2004) and (2) PGE deposits with disseminated sulphides (typically 0.5–5% sulphide; c.f. Barnes et al., 2017; Naldrett, 2004). This is a critical distinction, because the volume of sulphide liquid to silicate liquid in magmatic sulphide deposits is considered the first order control on the PGE tenor of ore (e.g. Campbell and Naldrett, 1979). Of the twenty-two "ultramafic" PGE occurrences documented in layered intrusions (Barnes et al., 2011; Kinnaird et al., 2017; Knight et al., 2011; Maier, 2005; Mansur and Ferreira Filho, 2016; Teixeira et al., 2015), only eight are truly "sulphide-poor" (with ≤10 vol. % disseminated sulphide) and confined to ultramafic host rocks (with >90 vol. % mafic minerals).

The eight sulphide-poor PGE occurrences within the ultramafic sequences of layered intrusions are documented in Table 2, in order of increasing sulphide content. We have excluded examples of PGE mineralisation in lamprophyric cumulates (Barnes et al., 2008), discordant dunite pipes (e.g. McDonald, 2008), Alaskan-type deposits (e.g. Thakurta et al., 2008) and similar concentrically-zoned intrusions

Table 2

A compilation of Volsprtuit-style mineralisation: sulphide-poor (≤ 10 vol% sulphide) PGE occurrences documented within the ultramafic portion of a layered intrusion.

Locality of PGE mineralisation	Lithology	Age	Max. vol. % sulphide in ore	Max. grade of mineralisation and/or defined deposit[a]	References
Sulphide Zone, Luanga Mafic-Ultramafic Complex, Serra Leste magmatic suite, Brazil	orthopyroxenite, harzburgite & peridotite	2763 Ma	< 3 vol %	1.24 ppm [“PGE+Au”]/142 Mt orebody	Mansur and Ferreira Filho, 2016; Mansur, 2017
Lago Grande Mafic-Ultramafic Complex, Serra Leste magmatic suite, Brazil	orthopyroxenite, harzburgite with <60 vol % chromite	2722 Ma	< 3 vol %	No information publically available	Teixeira et al., 2015
The Volspruit Sulphide Zone, Bushveld Complex, South Africa	orthopyroxenite (minor harzburgite), typically <15 vol. % chromite	~2056 Ma	< 3.6 vol % < 4 vol % [b]	5 ppm [Pt+Pd+Rh+Au]/4–16 m core[b] 1.23 ppm [Pt+Pd+Rh]/38.98 Mt	Hulbert and von Gruenewaldt, 1982; Venmyn, 2010; Cawthorn, 2015
NKT massif, Monchepluton, Monchegorsk Complex, Kola Region, Russia	lherzolite, harzburgite, olivine-websterite, orthopyroxenite, typically <1 vol. % chromite	~2445–2506 Ma	< 5 vol %	3.3 ppm [Pt+Pd]/3 m core	Karykowski, 2017; Karykowski et al., 2018
The Santa Rita deposit, Fazenda Mirabela Intrusion, Brazil	dunite, orthopyroxenite, harzburgite, typically <0.5 vol. % chromite	~2100 Ma	< 5 vol %	1.5 ppm [Pt+Pd]/1 m core 0.09 ppm [Pd]/121 Mt	Barnes et al., 2011; Knight et al., 2011
Ni-PGE ore in the Kevitsa Intrusion, northern Finland	olivine pyroxenite & websterite	2058 Ma	< 6 vol %	0.99 ppm [“PGE”]/290 m core 0.46 ppm [Pt+Pd+Au]/165 Mt	Le Vaillant et al., 2016; Scandinavian Minerals Limited, 2006; Yang et al., 2013; Söderholm, 2009
The Main Sulphide Zone, Great Dyke, Zimbabwe	pyroxenite & websterite	2575 Ma	< 10 vol %	5 ppm [“PGE”]/2–3 m core 3.75 ppm [Pt+Pd+Rh+Ru+Ir+Au] 1612 Mt (Ngezi mine)	Chaumba, 2017; Oberthür, 2011; Zientek et al., 2014
The Jinbaoshan ultramafic sill, Emeishan large igneous province, China	wehrlite, typically <10 vol. % chromite	259 Ma	< 10 vol %	5 ppm [Pt+Pd]/4–16 m core 3 ppm [Pt+Pd]/1 Mt	Tao et al., 2007; Wang et al., 2008; Wang et al., 2010

[a] These results report the concentration of PGE in the bulk rock, rather than the sulphide tenor of mineralisation normalised to 100% sulphide.

[b] Results reported in this study.

(e.g. Helmy and Mogessie, 2001) from the compilation presented in Table 2.

With the exception of the Jinbaoshan sill (259 Ma), these PGE occurrences are Paleoproterozoic or older. The proposed mechanism for PGE concentration in the localities listed in Table 2 involves sulphide saturation, formation of an immiscible sulphide melt and upgrading via equilibration between a small mass of immiscible sulphide liquid with a high mass of silicate melt (i.e. at a high R factor, c.f. Campbell and Naldrett, 1979). Proposed mechanisms to trigger sulphide melt saturation and/or increase the PGE tenor of the sulphide liquid include: fractional crystallisation of mafic silicates (e.g. Hulbert and von Gruenewaldt, 1982; Tao et al., 2007), fractional crystallisation of chromite (e.g. Hulbert and von Gruenewaldt, 1982; Tao et al., 2007), mixing of two compositionally distinct magmas (e.g. Hulbert and von Gruenewaldt, 1982), assimilation of country rock (e.g. Karykowski, 2017; Karykowski et al., 2018; Yang et al., 2013), temperature decrease during emplacement (e.g. Hulbert and von Gruenewaldt, 1982), involvement of/remobilisation by magmatic fluids (e.g. Chaumba, 2017; Knight et al., 2011; Teixeira et al., 2015) and multistage-dissolution upgrading (viz. Kerr and Leitch, 2005) by repeatedly resorbing sulphide liquid back into the silicate melt (e.g. Mansur and Ferreira Filho, 2016; Wang et al., 2010; Yang et al., 2013).

1.3.1. Mineralisation in the lower portions of layered mafic intrusions

While sulphide-poor PGE mineralisation in ultramafic cumulates constitutes ~7% of known PGE deposit styles, any economic or subeconomic mineralisation could deplete a fertile magma in PGEs. Thus ultramafic-hosted deposits have the potential to destroy the opportunity for other styles of PGE mineralisation higher up in the magmatic stratigraphy (c.f., Latypov et al., 2017), or in subsequent magma emplacement events sourced from the same reservoir (c.f., Mungall et al., 2016). A few detailed analytical studies of PGE distribution in sulphide-poor, ultramafic-hosted PGE deposits exist (e.g. Barnes et al., 2011; Diella et al., 1995; Gervilla and Kojonen, 2002; Grokhovskaya et al., 2012; Knight et al., 2011; Teixeira et al., 2015), but do not contain coupled studies comparing platinum-group mineral assemblages with the trace element chemistry of sulphides. Until now, few data have been available on the distribution of PGE and chalcophile trace elements from the Volspruit Sulphide Zone (e.g. Hulbert, 1983; Paktunc et al., 1990). By filling this knowledge gap, we hope to refine the genetic model for mineralisation in the lowermost portion of the Bushveld Complex. Understanding how and why fertile, primitive magmas achieve sulphide saturation in layered intrusions is crucial to understanding the formation of layered intrusions and guiding future mineral exploration.

2. Sampling and analytical techniques

To determine the mechanism(s) for ore genesis, we used nine pyroxenite samples from the Volspruit Sulphide Zone to (1) characterise high-density mineral assemblages (including platinum-group minerals), and (2) quantify the trace element chemistry of base metal sulphides.

Our methodology for identification of platinum-group minerals in sulphide ore differs from previous studies because:

(1) we systematically recorded all high-density minerals present in each sample (not just platinum-group minerals & electrum), and

(2) the texture of every high-density phase and the adjacent mineral assemblage were compiled and are provided as a visual atlas (Appendix A) and spreadsheet (Appendix B).

2.1. Samples

Nine samples of mineralised pyroxene ± chromite cumulates from the northern orebody of the Volspruit Sulphide Zone were taken from seven intervals between 67.88–121.88 m depth in the drill core GVN-042. Each sample is ~ 4 cm in length. By georeferencing the Fig. on page 8 of Pan Palladium Limited (2002), we estimate that the core GVN-042 was collared at 24°20′49.66″S, 28°56′54.13″E (the star shown in Fig. 1c) on the farm Volspruit 326KP. The location of centre-pivot irrigation systems around the drill-hole permit us to locate the drill core collar with reasonable accuracy (within a twenty-metre radius).

The nine drill core samples were impregnated with resin and prepared as rectangular polished blocks, with approximate dimensions of 20 x 30 x 3 mm. These samples are catalogued in the system for Earth sample registration (SESAR) database with international geo sample numbers (IGSN) from IEDDT0001-IEDDT0009. All depth values reported in the text are relative to the depth in the drillcore; they have not been corrected to account for dip. Core logs of GVN-042 were not provided with the samples, or available to the authors at the time of writing.

The mineralised pyroxene ± chromite cumulates used in this study were sampled across 53 m of drillcore. As the northern orebody is ~59 m thick in this area (Venmyn, 2010), these samples span from the top to the of the base of the Volspruit Sulphide Zone. Each thin section billet used in this study was only located within a 1 m interval of core GVN-042, corresponding to bulk geochemical assay data provided by Pan Palladium (Table 1). Therefore, the depth range of each sample is reported as a range (e.g. sample 7B = 67.88–68.88 m), but for convenience in figures, values are plotted as the mean of each depth range (e.g. sample 7B = 68.38 m).

2.2. Analytical techniques

2.2.1. Bulk rock geochemistry

The bulk rock geochemistry of one-metre intervals of drillcore was provided to us by Pan Palladium. The bulk geochemical data was determined by X-ray fluorescence for Ni, Cu, Cr and Sr; Rh, Pd, Pt and Au were determined by fire assay and inductively coupled plasma mass spectrometry.

2.2.2. Reflected light microscopy

Reflected light microscopy was used to record petrographic relationships in each polished block at 2.5x and 10x magnification, using a Nikon Optishot reflected light microscope at Cardiff University.

2.2.3. Electron microscopy: identification and characterisation of high-density minerals

A polished block from each stratigraphic level in the deposit was carbon-coated and examined for high-density minerals under the FEI XL30 field emission gun environmental scanning electron microscope (SEM) at Cardiff University. The perimeter of each polished rock surface was outlined using FEI software to facilitate sample navigation in the SEM. Analyses and back-scattered electron images were acquired at 20 kV with a nominal beam current of ~2 nA. Once the sample was in focus, the brightness and contrast of the back-scattered electron image were adjusted so that silicate, oxide and base metal sulphide minerals were black, and only minerals with a greater molar mass (and therefore,

greater density) were visible (e.g. platinum-group minerals and Pb-minerals). Each sample was then systematically searched for high-density minerals at 350x magnification by conducting manual y-axis traverses across the stage at a moderate scanning speed (1.68 ms per line with 968 lines per frame). Once a high-density mineral was found, it was imaged and analysed semi-quantitatively using an Oxford Instruments X-act energy dispersive spectrometer (EDS) and Inca X-ray analysis system. The brightness and contrast were recorded and briefly readjusted to image and analyse the adjacent mineral assemblage surrounding each high-density mineral. All visible minerals observed using this method were recorded and presented in Appendixes A and B.

To collect additional analyses and back-scattered electron images, we used a bench-top Phenom XL scanning electron microscope with a built-in EDS detector at the University of Wollongong.

2.2.4. Trace element chemistry of base metal sulphides

Trace element contents of base metal sulphide minerals were analysed *in situ*, in each of the nine samples using laser ablation inductively coupled plasma mass spectrometry (LA-ICP-MS). Relative abundances of trace elements were determined by ablating traverses (40 μm diameter wide; 300 μm long) at 6 μm/sec across base metal sulphide grains. We used a New Wave Research UP213 UV laser system coupled to a Thermo X series 2 ICP-MS housed at Cardiff University, following the methods described by Prichard et al. (2013) and Smith et al. (2014).

Given the fine grain size of sulphides analysed in this study, regions of the traverse containing mixed peaks from co-ablation of silicate, oxide, other sulphide or platinum-group minerals were excluded. The following isotopes were measured: ^{24}Mg, ^{29}Si, ^{33}S, ^{47}Ti, ^{52}Cr, ^{57}Fe, ^{59}Co, ^{60}Ni, ^{65}Cu, ^{66}Zn, ^{68}Zn, ^{72}Ge, ^{75}As, ^{77}Se, ^{82}Se, ^{83}Kr, ^{99}Ru, ^{101}Ru, ^{103}Rh, ^{105}Pd, ^{106}Pd, ^{108}Pd, ^{109}Ag, ^{111}Cd, ^{118}Sn, ^{121}Sb, ^{125}Te, ^{185}Re, ^{187}Os, ^{189}Os, ^{193}Ir, ^{195}Pt, ^{197}Au, ^{206}Pb and ^{209}Bi. Internal standardisation was based on ^{33}S using stoichiometric values for pentlandite (33 wt% S), pyrrhotite (38 wt% S) and chalcopyrite (35 wt% S), as these were the only minerals observed in our study.

The reference material CANMET Po724 (a synthetic FeS doped with ~40 ppm PGEs and Au) was measured to monitor the relative standard deviation (RSD) of analyses (Appendix C). Our results fall within reported values from published literature, with the exception of ^{106}Pd, ^{108}Pd and ^{209}Bi, where few values have been reported. Analyses of PGEs & Au were < 9% RSD.

For elements where multiple isotopes were analysed (Zn, Se, Ru & Pd), we preferentially use the isotopes ^{68}Zn, ^{77}Se, ^{101}Ru and ^{106}Pd. Ar and He gases used during LA-ICP-MS analysis may contain ^{82}Kr, creating a potential isobaric interference with ^{82}Se.

3. Results

3.1. Bulk rock chemistry

The bulk rock chemistry of one-metre drillcore intervals from the northern orebody of the Volspruit Sulphide Zone is provided in Table 1. These data demonstrate that our samples are high-grade relative to the resource estimate for the northern orebody, with a maximum grade of 5 ppm (Pt + Pd + Rh + Au) from 115.88–116.88 m depth. The mean grade of Ni, Pt and Pd in the northern Volspruit Sulphide Zone is comparable with Platreef and GNPA-hosted mineralisation, but contains significantly reduced grades of Cu and Au (Table 1).

3.2. Petrologic features of orthopyroxenites in the Volspruit Sulphide Zone

The mineralised cumulates from the Volspruit Sulphide Zone are medium-grained chromite orthopyroxenites and orthopyroxenites (viz. Maître et al., 2002), showing variable degrees of serpentinisation (Fig. 4; Fig. 5a-i). Orthopyroxene is subhedral, with a grain size typically 0.2–3 mm, but with grains up to 5 mm in the sample at 115.88–
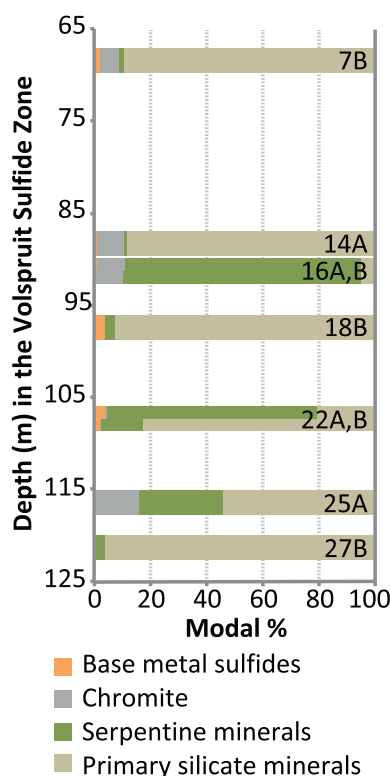
Fig. 4. Variation in the modal abundance of minerals with depth in the Volspruit Sulphide Zone. The modal proportion of minerals was visually estimated under reflected light using nine polished blocks from seven intervals in the GVN-042 drill core, intersecting the Volspruit Sulphide Zone.

116.88 m depth. Samples contain 5–96 vol. % orthopyroxene, 0.5–15% chromite, 0.3–4% base metal sulphides and 1–85% serpentine minerals (Appendix D; Fig. 4). In each sample, orthopyroxene is crosscut and replaced by serpentine veinlets. Given the high degree of serpentinisation in some samples (e.g. Figs. 4 and 5), it is possible that either olivine or clinopyroxene could have been a precursor silicate mineral to serpentinite, rather than orthopyroxene. However, relict olivine or clinopyroxene are rarely observed under electron microscopy. Serpentine minerals are observed infilling fractures up to 0.5 mm wide. The sample at 106.88–107.88 m depth (Figs. 4–5) demonstrates that there is variability in the degree of serpentinisation within one-metre intervals of the Volspruit Sulphide Zone. Pervasive serpentinisation at the micrometer-scale is evident in all samples, with alteration typically occuring at the margin between base metal sulphides and adjacent orthopyroxene. Many base metal sulphide assemblages exhibit altered margins, with sulphide minerals replaced by serpentine minerals.

As well as identifying the mineralogy of high-density mineral assemblages in the Volspruit Sulphide Zone, electron microscopy of petrological relationships surrounding the high-density assemblages revealed: (1) sub-rounded to spherical inclusions hosting exotic[5] phases within chromite, (2) the presence of exotic microxenocrysts (<300 μm diameter) in the pyroxenite matrix, and (3) base metal sulphide assemblages atypical of sulphide-poor PGE mineralisation.

3.2.1. Chromite-hosted inclusions

Silicate, carbonate and sulphide inclusions are observed within chromite crystals, with differences in the inclusion density between samples (Fig. 6a-h). These inclusions typically occur within the core of chromite grains, rather than the rim. They are either sub-rounded, rounded, or have faceted margins that may be negative crystal shapes. The texture

of host chromite ranges from isolated euhedral-subhedral crystals, to chains of chromite, equigranular chromite aggregates and amoeboidal chromites.

The proportion of chromite grains containing inclusions ranges from 5–60%. Of the grains bearing inclusions, the inclusion density ranges from 1–10 inclusions per grain. Samples with a higher percentage of chromite grains containing inclusions also exhibit the greatest density of inclusions per grain (i.e. the sample in which 60 vol. % of chromites have one or more inclusion contain chromite crystals bearing up to 10 silicate inclusions per grain; Appendix D). While there is no pattern with the vol. % chromite against depth in the Volspruit Sulphide Zone, the most striking feature of these data is that the percentage of chromite grains containing inclusions increases with height in the Volspruit Sulphide Zone – from 8% of chromite grains bearing inclusions at the base of the Volspruit Sulphide Zone (120.88–121.88 m depth), to 60% near the top (87.88–88.88 m depth) (Appendix D). The topmost sample of the Volspruit Sulphide Zone is the one exception, with only 5% of grains containing inclusions at 67.88–68.88 m depth.

The mineral assemblages that characterise the silicate inclusions in chromite are different from those found in pyroxenite in the Volspruit subzone. Orthopyroxene was not observed in any of the inclusions analysed. Instead, inclusions in chromite contain a range of exotic, more felsic and occasionally hydrous silicate and aluminosilicate phases such as albite, (Ca,K,Na)-Al-Si-Cl-O, and (Mg,Fe)-Al-Si-O (Fig. 6). High-density minerals including (La,Ce)-monazite and Pb-chlorides are also observed in silicate inclusions, hosted within chromite.

One subhedral chromite-hosted carbonate inclusion was observed at 115.88–116.88 m depth (Fig. 7e). This inclusion contains Ca-Mg carbonate (i.e., dolomite) with trace Sr and Fe, with magnetite on one margin of the chromite inclusion. As magnetite was only observed at the boundary between the host chromite and dolomite, we infer that the magnetite grew after entrapment, so it is likely of secondary origin.

Base metal sulphide inclusions in chromite are observed in two samples. At 90.88–91.88 m depth (Fig. 6d), a small bleb[6] composed of pentlandite and pyrrhotite occurs in association with albite and a possibly hydrated aluminosilicate. At 115.88–116.88 m depth, seven sulphide inclusions are documented within one chain of chromite crystals (Fig. 5h).

The sample at 90.88–91.88 m depth contains one 8 μm base metal sulphide bleb composed of pyrrhotite and pentlandite within a polymineralic chromite-hosted silicate inclusion (Fig. 6d). This bleb is attached to the chromite-inclusion boundary. The silicate inclusion hosting the sulphide bleb contains hydrous felsic aluminosilicate minerals, albite and one monazite grain.

In the chain of seven sulphide inclusions at 115.88–116.88 m depth, four inclusions contain base metal sulphide assemblages, while three contain a mixture of sulphide and silicate minerals. Outside this one chain of chromite crystals, sulphide inclusions are not observed elsewhere in the sample. This sample contains a low proportion of silicate inclusions in chromite (8 vol. %) but exhibits the highest grade of ore and greater Pt/Pd compared to other samples from the Volspruit Sulphide Zone (Table 1).

In the sulphide-only inclusions, pyrrhotite is the dominant mineral, with pentlandite, magnetite and minor chalcopyrite. In one sulphide inclusion, flames of Fe-rich pyrrhotite were observed amongst Fe-poor pyrrhotite (Fig. 6h). Three-quarters of sulphide-rich inclusions contain sperrylite ($PtAs_2$) too fine to observe using systematic high-density mineral identification at 350x magnification. The largest high-density mineral within a chromite-hosted sulphide inclusion was an elongate 0.9 x 0.2 μm sperrylite inclusion (Fig. 6f). Sperrylite occurs at the contact between sulphides (pyrrhotite, pentlandite and chalcopyrite) and enclosing chromite (Fig. 6). In only one case, sperrylite was observed

---

[5] Here, we use the term exotic to describe minerals considered atypical in pyroxenite.

[6] Here, we use the term bleb as defined by Barnes et al., (2017, page 475) as "a composite aggregate, at a scale from tens of micrometres to a few centimetres, regardless of its textural relationship to associated gangue silicate phases".
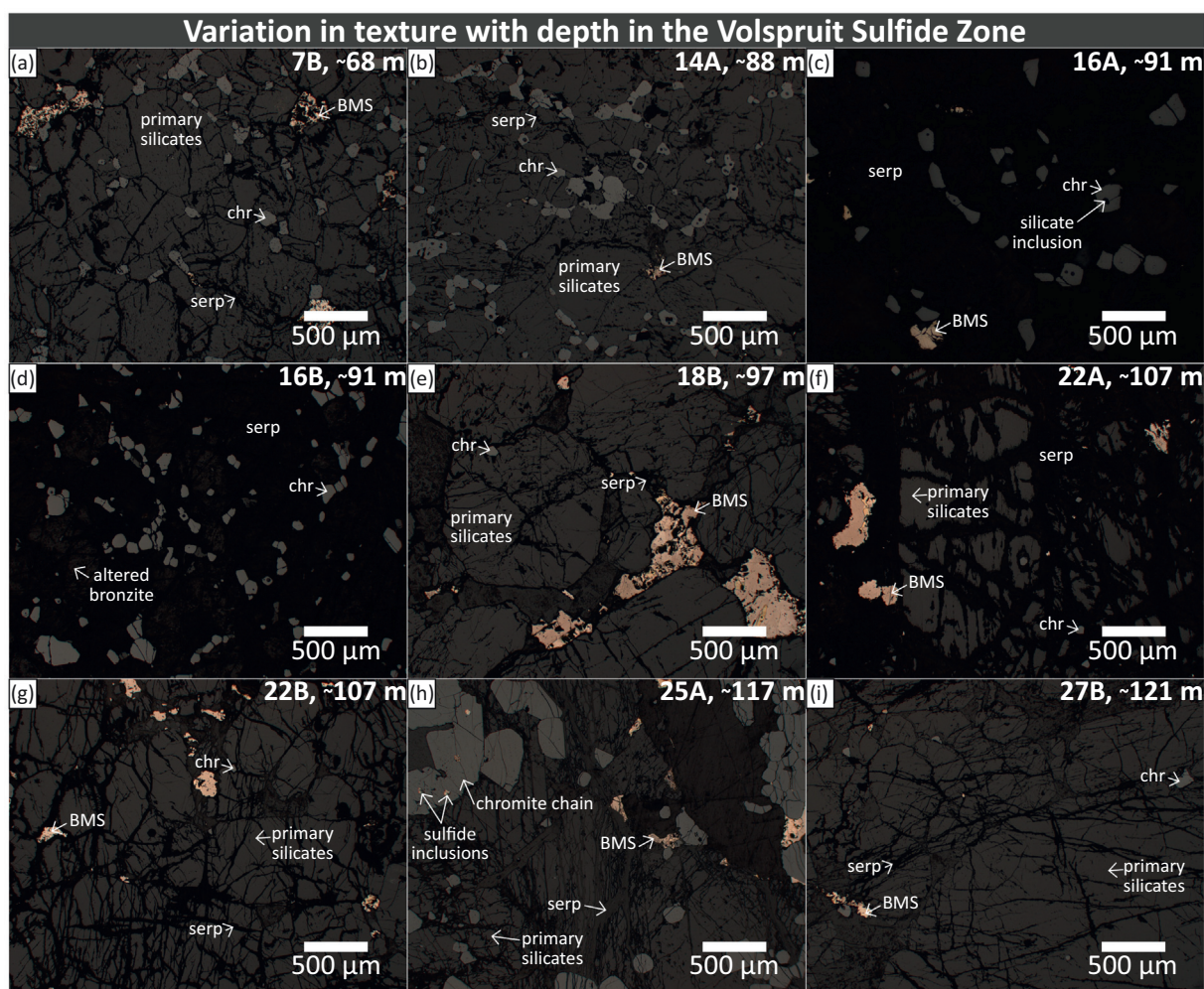
Fig. 5. Reflected light photographs from each of the nine polished blocks used in this study, documenting the range in texture with depth in the Volspruit Sulphide Zone. BMS = base metal sulphides, chr = chromite, serp = serpentine minerals.

away from the inclusion margin, at a pentlandite-pyrrhotite grain boundary.

In the three sulphide-silicate inclusions, Pb-chlorides and Pb-sulphides were observed in association with pyrrhotite, magnetite and hydrated Fe-Mg silicates such as phlogopite. In both the silicate-sulphide inclusions and the sulphide-only inclusions, magnetite is only observed at the boundary between chromite and pyrrhotite, so it likely formed post-entrapment.

3.2.2. Microxenocrysts

Electron microscopy revealed exotic minerals less than 300 μm in diameter: $CaCO_3$ (at 106.88–107.88 m), Mn-rich ilmenite ($ilmenite_{76}$-$pyrophanite_{24}$; at 106.88–107.88 m) and U–Pb-Th oxide (120.88–121.88 m depth) (Fig. 8a-c). Because these minerals (1) occur within the pyroxenite matrix, but are atypical of ultramafic mineral assemblages, and (2) do not display interstitial textures suggestive of late-crystallising phases, we interpret these exotic minerals as microxenocrysts. Neither xenoliths nor xenocrysts are evident in samples from the Volspruit Sulphide Zone under reflected light. Baddeleyite and titanite were also documented (Fig. 8), but these are less likely to be xenocrysts.

3.2.3. Atypical magmatic sulphide assemblages

Under reflected light microscopy, disseminated blebs of pyrrhotite, pentlandite and chalcopyrite show no unusual characteristics. Typical base metal sulphide assemblages occur as blebs containing

intergrowths of pyrrhotite, pentlandite, chalcopyrite and cubanite, but these minerals also infill fractures in chromite and are included within chromite. Electron microscopy revealed that some magmatic sulphide assemblages were accompanied by a suite of accessory Pb- and Zn-minerals atypical of magmatic sulphide deposits (cf. Naldrett, 2004).

Fig. 9a-f demonstrates that base metal sulphide assemblages include accessory sphalerite, Pb-sulphide minerals (± minor Se, Cl) and a suite of Pb-chloride minerals (± K, S, Se, Te). While sphalerite and Pb-minerals are not exclusively hosted within base metal sulphide assemblages, it is significant for the genesis of the Volspruit Sulphide Zone that many are, as they appear to be primary inclusions.

Unlike the Pb-minerals, sphalerite is not a high-density phase that is easily distinguished under back-scattered electron imaging; only two occurrences are observed – although they may be more prevalent than we have documented. In one instance at 106.88–107.88 m depth (the sample containing the highest number of included Pb-sulphides and Pb-chlorides), sphalerite is included in the centre of a base metal sulphide bleb. Fig. 9b shows the ~125 $μm^2$ sphalerite grain with curvilinear to cuspate margins bounded by pyrrhotite and chalcopyrite. We interpret this image as primary sphalerite, crystallising in the remaining space against the already solidified pyrrhotite. In the same sample, there is a second occurrence of sphalerite with a more ambiguous origin, with relict sphalerite (<4 $μm^2$), chalcopyrite and pentlandite trapped within the cleavage of a blocky Se-bearing galena crystal (Fig. 9c).
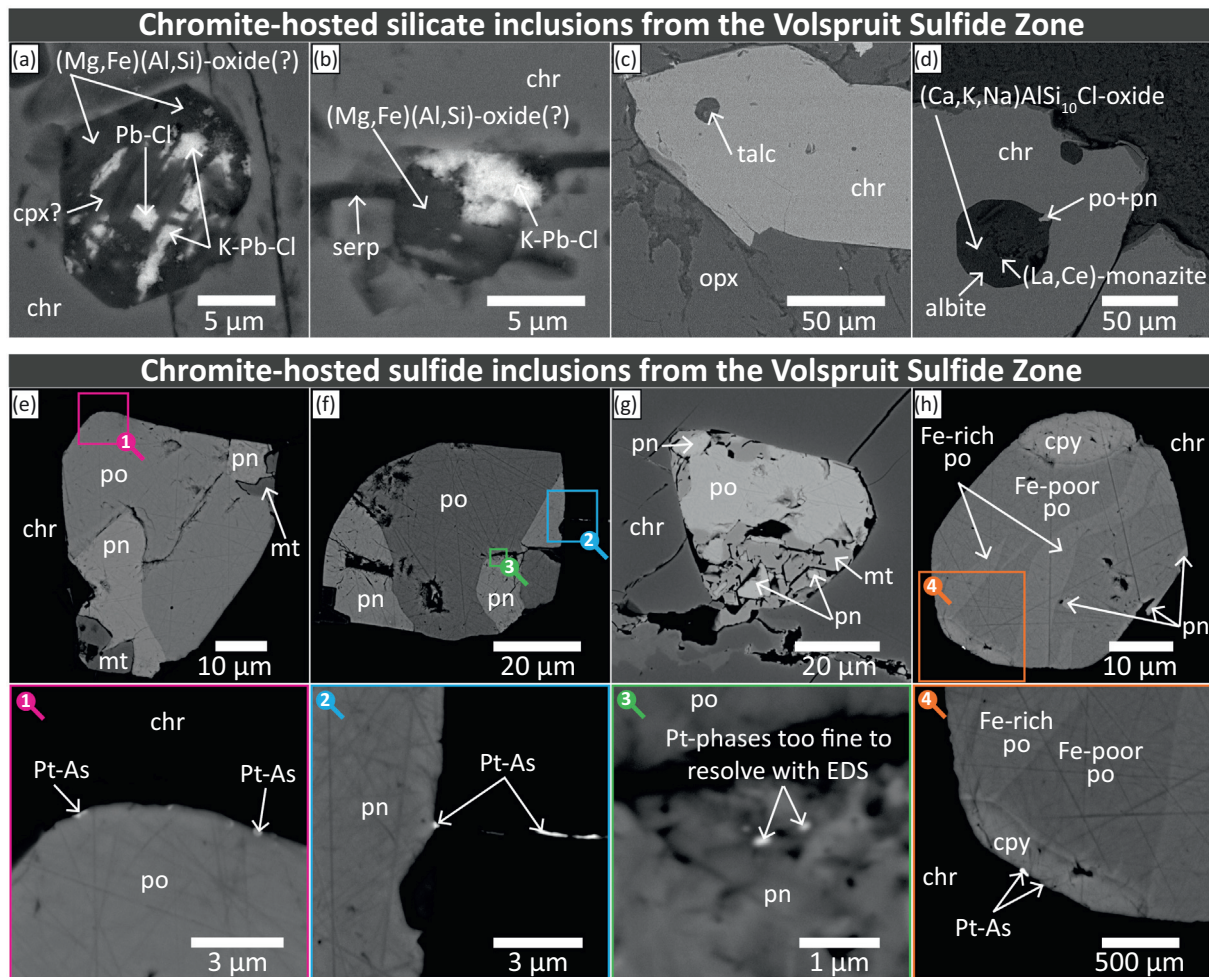
Fig. 6. Back-scattered electron images of chromite-hosted silicate and sulphide inclusions from the Volspruit Sulphide Zone. Cpx = clinopyroxene, chr = chromite, serp = serpentine minerals, opx = orthopyroxene, po = pyrrhotite, pn = pentlandite, mt = magnetite, cpy = chalcopyrite. Coloured insets 1–4 below figures e-h show the corresponding images at higher magnification.

Accessory Pb-sulphide and Pb-chloride minerals are *included within* base metal sulphide assemblages at four depth intervals of the Volspruit Sulphide Zone (samples from 87.88–88.88 m, 90.88–91.88 m, 106.88–107.88 m & 115.88–116.88 m depth). For example, galena (with detectable Se using EDS analysis) occurs as rounded inclusions up to 60 μm in diameter within pyrrhotite (Fig. 9a). Fig. 8a shows both Pb-chloride and Pb-sulphide included within the same sulphide bleb. As Pb-minerals are high density, a more complete analysis of Pb-sulphide and Pb-chloride minerals is presented below.

3.3. Quantification and characterisation of high-density mineral assemblages

A total area of 32.895 cm^2 of pyroxenite cumulates were searched for high-density minerals, identifying 0.00027 area % high density phases. The high-density mineral assemblage in the Volspruit Sulphide Zone contains: 196 precious metal mineral grains (Pt-, Pd-, Rh-, Au- or Ag-minerals; 24 area %), 126 Pb-mineral grains (76 area %), and 2 exotic mineral grains (<0.1 area %) (Fig. 10). These data are available to download electronically in Appendix B. Below, we report the results of the precious metal mineral assemblages and Pb-minerals separately. Precious metal minerals are only observed in close association with Pb-minerals in three instances (Fig. 9d-f). The two exotic high-density

minerals, (La-Ce) monazite and U-Th-Pb oxide (Fig. 8) are both interpreted as microxenocrysts, as discussed above.

3.3.1. Characterisation of precious metal minerals

The 196 precious metal mineral grains range in size from 0.25–180 μm^2 and contain a diverse range of compositions. Pt, Pd, Ag, Au and Rh are the dominant cations, typically forming complexes with one or more of the following anions: Te, Bi, As, Fe, S, Sn or Sb. In order of decreasing modal abundance, precious minerals identified in the Volspruit Sulphide Zone include: Pt-bismuthotellurides, Pd-bismuthotellurides, Pt-alloys, Pt-bismuthides, Pt-arsenide, Pt-arsenosulphide, electrum (Au-Ag), (Pt, Pd)-bismuthotellurides, Ag-telluride, (Pt-Rh)-arsenosulphide (Fig. 7a-f). Other precious metal minerals constitute <15 μm^2 in area. Pt and Pd-sulphides are notably absent from this assemblage.

The abundance of precious metal minerals varies with height in the Volspruit Sulphide Zone (Fig. 10). However, there are no systematic mineralogical trends with depth in the core. The Pt/Pd of precious metal minerals oscillates above and below 1 throughout the Volspruit Sulphide Zone, with no systematic trend. Instead, some horizons are punctuated with a greater diversity of precious metal minerals. For example, Fe-alloys are most dominant in the sample at 96.88–97.88 m depth with the highest volume of precious metal minerals and Rh only occurs in the sample at 115.88–116.88 m depth with the highest volume of arsenides and sulfarsenides.
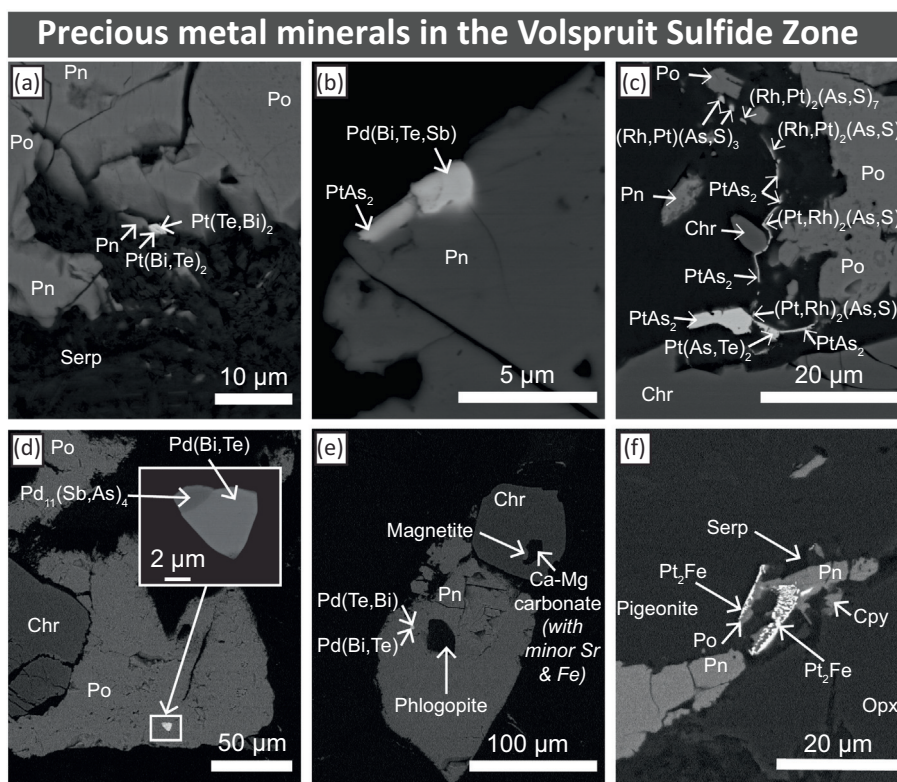
Precious metal minerals in the Volspruit Sulfide Zone

Fig. 7. Selected back-scattered electron images of high-density precious metal minerals from the Volspruit Sulphide Zone. Po = pyrrhotite, pn = pentlandite, serp = serpentine minerals, chr = chromite, opx = orthopyroxene, cpy = chalcopyrite. Please refer to Appendix A for a complete annotated visual atlas of high-density minerals collected in this study.
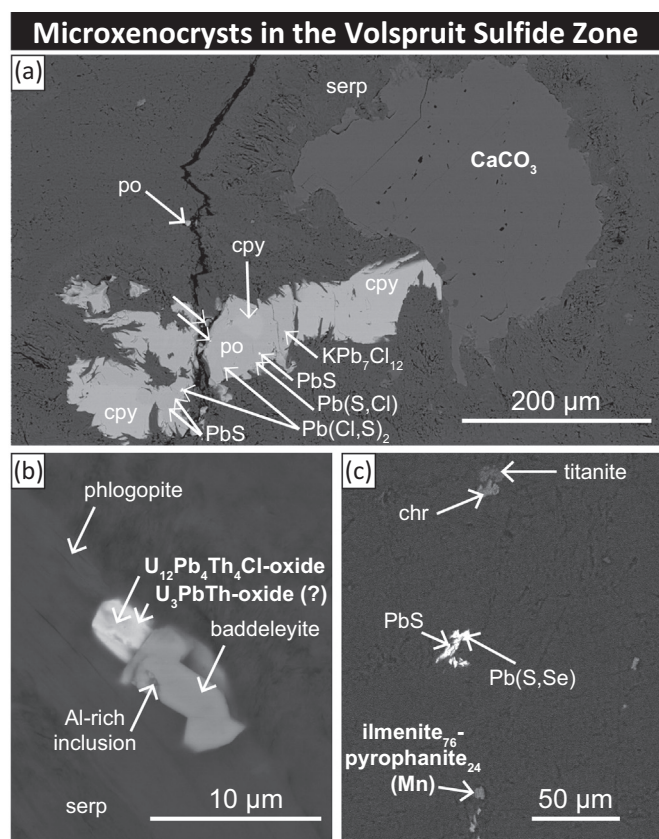
Microxenocrysts in the Volspruit Sulfide Zone

Fig. 8. Back-scattered electron images of minerals interpreted as microxenocrysts (highlighted in bold text) from the Volspruit Sulphide Zone. Po = pyrrhotite, cpy = chalcopyrite, serp = serpentine minerals, chr = chromite.

Precious metal minerals were observed in a variety of host assemblages (Fig. 11), with textures ranging from spongy, symplectic to euhedral. Of the 196 precious metal mineral grains identified, 39% are enclosed within serpentinite near[7] altered base metal sulphide(s), 29% are at the altered grain boundary between base metal sulphide(s) and silicate(s), 10% are enclosed within base metal sulphide, and 8% are enclosed within serpentinite. The remainder of assemblages occur at altered grain boundaries between base metal sulphide, silicate and chromite (4%), grain boundaries between serpentine and pyroxene near altered base metal sulphide (4%) and in the absence of base metal sulphide (4%), altered silicate-chromite grain boundaries (1%) and enclosed within silicates in fractured chromite (0.5%).

Precious metal minerals either occur as individual phases or as intergrowths with more than one mineral (Fig. 7). Two assemblages contain clear core-rim relationships, with $Pd(Bi,Te,Sb)$ overgrowing a cylindrical core of $PtAs_2$ at the margin of a pentlandite grain (Fig. 7b) at 106.88–107.88 m depth and $Pt(Te,Bi)_2$ overgrowing $Pd(Te,Bi)$, nucleating from a clinopyroxene at 67.88–68.88 m depth. Fe-alloys were the only precious metal mineral assemblages to exhibit symplectic textures (Fig. 7f). Sponge-like textures were evident in a few instances at 120.88–121.88 m depth and at 67.88–68.88 m depth.

The primary precious metal minerals included within magmatic sulphide blebs are enclosed within pyrrhotite, pentlandite or chalcopyrite. Pyrrhotite contains primary inclusions of $Pd(Bi,Te)$ (6 grains), $Pd_2(Te,Bi)$, $Pd_3(BiTe)_2$, Pd_3Te, $(Pd,Pt)_3Sn$, $Pd_{11}(Sb,As)_4$ and $Pt(Te,Bi)_2$. Pentlandite contains primary inclusions of electrum (Au-Ag), $(Pd,Pt)Bi$, $Pd(Bi,Te)$, Pt_2Te and $Pt(Te,Bi)$. Chalcopyrite contained primary inclusions of $(Pd,Pt)(Bi,Te)_2$ and $Pt(Te,Bi)_2$.
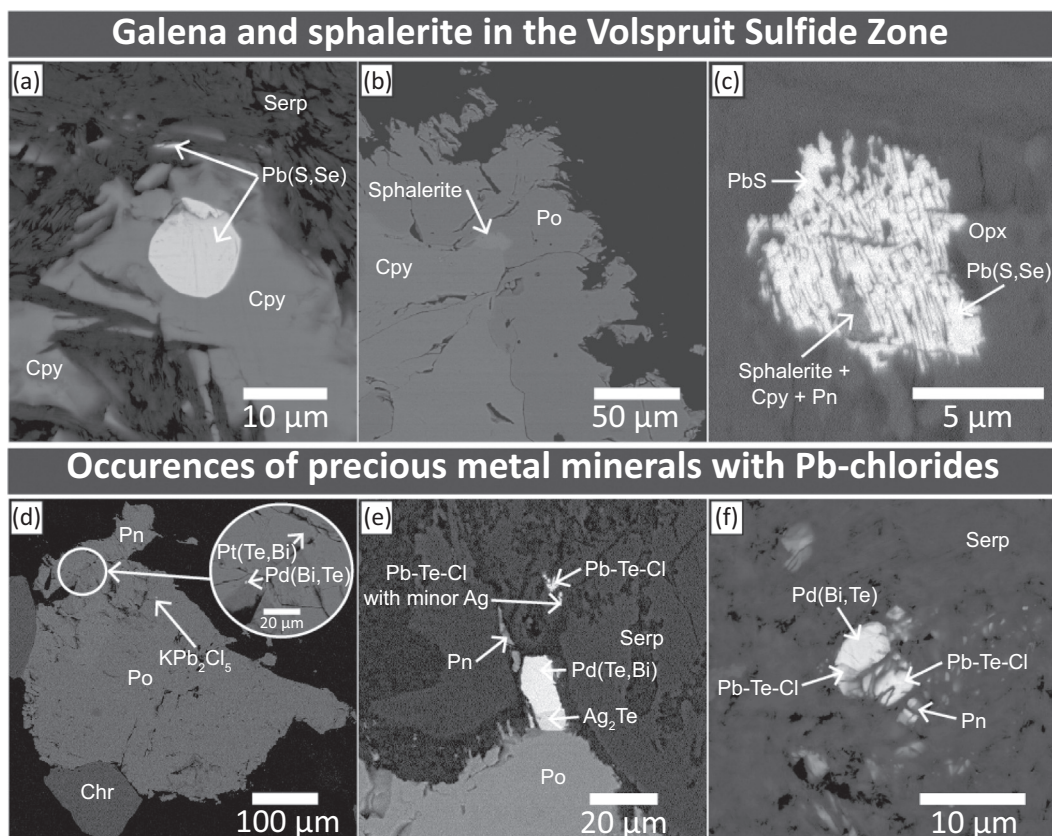

Fig. 9. Back-scattered electron images of Pb and Zn minerals associated with magmatic sulphide assemblages (a-c) and precious metal mineral assemblages (D-F) from the Volspruit Sulphide Zone. Serp = serpentine minerals, cpy = chalcopyrite, po = pyrrhotite, pn = pentlandite, opx = orthopyroxene, chr = chromite.

3.3.2. Characterisation of Pb-minerals

Pb-minerals were observed at each of the seven intervals from the Volspruit Sulphide Zone. Of the 126 Pb-mineral grains observed in this study, 98 grains (92 area%) were Pb-sulphides (± Se, Cl) and 27 grains (7 area%) were Pb-chlorides (± K, Se, Te, S); grain size ranges from 0.25–1950 μm^2. Pb-Te-chlorides were observed in two instances, associated with precious metal assemblages (Fig. 9e-f). Pb-minerals dominate high-density mineral assemblages at 90.88–91.88 m depth and 106.88–107.88 m depth in the Volspruit Sulphide Zone, where Pb is dominantly hosted by Pb-sulphides. Fig. 10 shows that while Pb-sulphides are more abundant overall, they were only observed at four out of seven depth intervals. While Pb-chlorides were less abundant, they were observed at six out of seven depth intervals.

Pb mineral assemblages exhibit a range of textural associations (Fig. 11). Of the 125 Pb-minerals, 50% of these are enclosed within serpentinite. 20% occur within serpentinite near altered base metal sulphide assemblages. 8% are enclosed in base metal sulphide assemblages, while 5% occur at altered grain boundaries between base metal sulphide(s)and silicate(s). The remainder occur at serpentine-pyroxene grain boundaries (sometimes near altered sulphide), enclosed within chromite-hosted silicate inclusions, enclosed within altered base metal sulphide assemblages in fractured chromite, enclosed within silicate(s) in fractured chromite, enclosed within pyroxene and at altered triple junctions between silicate-chromite-base metal sulphide(s).

Half the Pb-sulphide minerals observed in this study have blocky/graphic textures. Nine out of the ten K-Pb-chlorides, as well as two Pb-chloride grains and four Pb-sulphide grains exhibit a spongy texture. Otherwise, Pb-minerals are typically homogenous.

Primary Pb-sulphides and Pb-chlorides are enclosed within pyrrhotite, pentlandite, chalcopyrite, pyroxene or chromite-hosted silicate inclusions. In one instance at 106.88–107.88 m depth, an inclusion of Pb(Cl,Se) was observed in Pb(S,Se), enclosed within pyrrhotite. Pyrrhotite hosts primary inclusions of KPb_2Cl_5, KPb_7Cl_{12}, Pb(S,Se), PbS (seven grains), Pb_2Cl and PbCl. Pentlandite hosts four primary
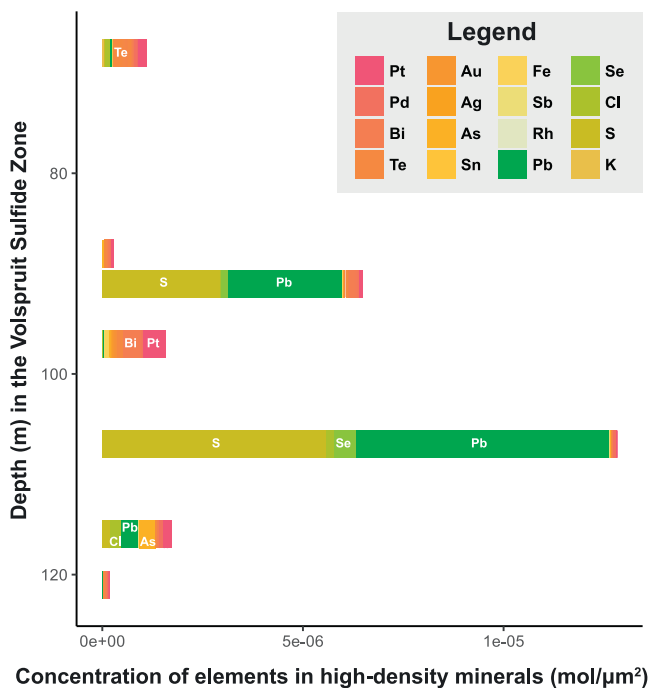

Fig. 10. Variation in the composition and abundance of high-density minerals with depth in the Volspruit Sulphide Zone.
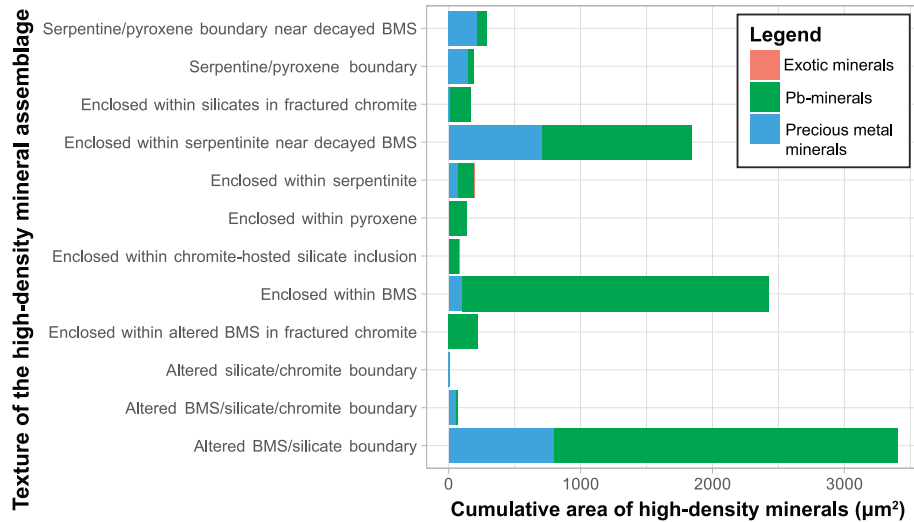
Fig. 11. Location and textural association of high-density minerals in the Volspruit Sulphide Zone.

Table 3
Range of tenors and S/Se values in base metal sulphides from the Volspruit Sulphide Zone. The complete dataset for all trace elements in base metal sulphides is presented as a spreadsheet in Appendix E.

	Depth (m)	n=	^{101}Ru (ppm)	^{189}Os (ppm)	^{193}Ir (ppm)	^{103}Rh (ppm)	^{195}Pt (ppm)	^{106}Pd (ppm)	^{109}Ag (ppm)	^{33}S/^{77}Se	3PGE + Au
Chalcopyrite	90.88–91.88	2	bdl- 0.1	bdl	bdl	bdl	bdl	0.5–0.8	11.9–66.2	3,377 - 3,850	0.5–0.8
	96.88–97.88	1	bdl	bdl	bdl	bdl	bdl	0.2	5.0	6,804	0.2
	115.88–116.88	1	bdl- 0.2	bdl	bdl	bdl	bdl	bdl	3.1	5,264	bdl
Cubanite	106.88–107.88	1	bdl	bdl	bdl	bdl	bdl	bdl	0.7	7,858	0.1
Pentlandite	87.88–88.88	2	5.9–8.5	2.2–2.3	1.7–2.6	14.2–18.9	0.1–0.3	216.5–244.0	0.9–7.3	3,099 - 3,875	235.5–258.4
	90.88–91.88	7	2.7–5.7	0.5–1.9	1.3–1.8	7.8–19.3	0.1–0.8	116.1–227.8	1.7–18.5	1,405 - 3,202	124.6–236.8
	106.88–107.88	3	0.7–6.3	0.3–1.3	0.2–2.4	1.4–50.8	bdl- 0.2	39.3–61.4	1.6–2.2	3,520 - 5,277	40.9–112.4
	120.88–121.88	3	bdl- 2.6	0.2–0.9	0.1–0.5	0.4–6.5	bdl	49.3–90.9	1.0–6.0	4,372 - 5,715	51.8–91.3
Pyrrhotite	67.88–68.88	5	bdl- 1.9	0.3–0.7	0.1–0.3	bdl	bdl	bdl- 0.1	bdl- 0.2	4,899 - 5,281	bdl- 0.1
	87.88–88.88	3	bdl- 3.1	0.1–1.2	bdl- 0.6	bdl- 0.2	bdl- 0.7	bdl- 1.3	bdl- 0.2	4,136 - 5,139	0.1–1.6
	90.88–91.88	1	0.2	bdl	bdl	bdl	0.5	bdl	0.5	4,405	0.6
	96.88–97.88	10	0.2–2.0	bdl- 0.8	0.1–0.6	bdl- 0.7	bdl- 1.2	bdl- 0.1	bdl- 0.3	5,835 - 10,480	bdl- 2.0
	106.88–107.88	17	bdl- 2.6	bdl- 0.8	bdl- 1.0	bdl- 0.4	bdl- 0.3	bdl- 0.1	0.1–0.5	4,842 - 8,990	bdl- 0.9
	115.88–116.88	10	bdl- 2.4	0.1–1.0	bdl- 0.5	bdl- 0.8	bdl- 0.1	bdl- 0.3	bdl- 1.0	4,371 - 18,972	bdl- 1.2
	120.88–121.88	8	bdl- 7.2	bdl- 1.1	bdl- 1.6	bdl- 29.6	bdl- 6.1	bdl- 0.2	bdl- 0.7	6,360 - 21,566	bdl- 35.7

inclusions of Pb(S,Se). Chalcopyrite hosts primary inclusions of Pb(Cl, S), Pb(S,Se) and Pb(S,Cl,Se). Pyroxene enclosed two grains of PbS and three grains of Pb(S,Se). While some inclusions are fractured and thus may be altered by secondary processes, chromite-hosted silicate inclusions contain a range of K-Pb-Cl (5 grains) and PbCl$_2$ (e.g. Fig. 6a-b).

3.4. Trace element chemistry of base metal sulphides

LA-ICP-MS traverses across pyrrhotite, pentlandite, chalcopyrite and cubanite demonstrate that a range of precious metals and semi-metals are concentrated within base metal sulphides in the Volspruit Sulphide Zone. These data are available to download in Appendix E, are summarised in Table 3 and are plotted against depth in the Volspruit Sulphide Zone in Fig. 12. Due to the small size of base metal sulphides and fine intergrowths between different sulphide phases in the Volspruit Sulphide Zone, pure trace element analyses[8] could not be obtained for each mineral at every depth. A lack of

suitable reference materials meant that some trace metals such as Pb could not be measured. Nevertheless, we measured a diverse range of trace metals in sulphides from the Volspruit Sulphide Zone, which reveal critical information about the distribution of platinum-group elements and semi-metals between minerals in base metal sulphide assemblages.

3.4.1. Concentration of precious metals in base metal sulphides

Most notably, magmatic sulphide assemblages in the Volspruit Sulphide Zone achieve extremely high tenors, with up to 251 ppm (Pt + Pd + Rh + Au) in pentlandite from 87.88–88.88 m depth. However, there is a significant range of tenors within minerals from the same depth interval. For example, pentlandite at 90.88–91.88 m depth contains 115–222 ppm Pd and 8–19 ppm Rh. The highest concentration of PGEs in pentlandite at 87.88–88.88 m depth is defined by 236 ppm Pd, 14 ppm Rh, 6 ppm Ru, 2 ppm Ir and 2 ppm Os. While Ru is primarily concentrated in pentlandite, pyrrhotite also contains consistently high tenors, with up to 8 ppm Ru.

Pentlandite and pyrrhotite typically contain ≤1 ppm Pt, with the exception of pyrrhotite at 120.88–121.88 m depth containing 4–6 ppm Pt. Pyrrhotite at 120.88–121.88 m depth is also enriched in Rh, Ru, Ir and Os (Fig. 12). Chalcopyrite contains the highest Ag concentrations (up to 66 ppm), although Ag concentrations can reach up to 18 ppm in

---

[8] The results of mixed analyses (e.g. pyrrhotite-pentlandite) are presented in Appendix E as information values only. Because the exact ratio of two phases is not known, we could not correct for the internal standard (^{33}S), thus producing inaccurate trace element concentrations. Therefore, mixed analyses are not considered in this study.
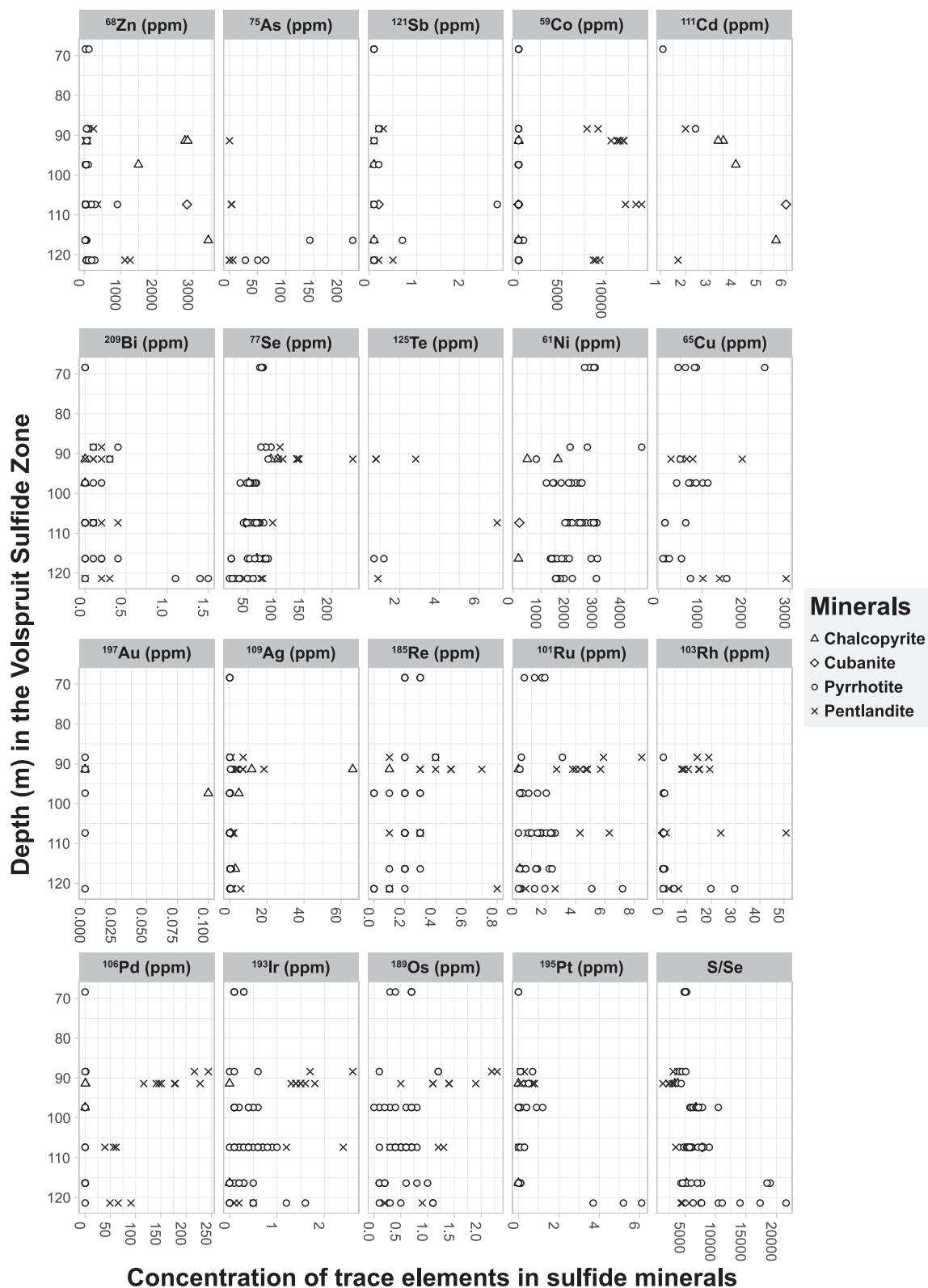
Fig. 12. Variation in the trace element chemistry of base metals sulphide minerals (chalcopyrite, cubanite, pyrrhotite and pentlandite) with depth in the Volspruit Sulphide Zone.

pentlandite. By contrast, Au occurs at <0.06 ppm in all base metal sulphides analysed in this study.

3.4.2. Concentration of other trace elements within base metal sulphides

Base metal sulphides in the Volspruit Sulphide Zone are important reservoirs for a suite of trace metals including (in order of decreasing abundance) Co, Zn, Se, As, Te, Cd, Sb and Bi. Just like the precious metals, these trace metals may exhibit a wide range of concentrations within minerals from the same depth interval; e.g., pentlandite from 90.88–91.88 m depth contains 104–237 ppm Se. Pentlandite is the primary host of Co (up to 1.4 wt%), Se (up to 237 ppm) and Te (up to 7 ppm); chalcopyrite is the primary host of Zn (up to 3,416 ppm); Cd is most

concentrated in cubanite (up to 6 ppm). While two grains of sphalerite were observed at 106.88–107.88 m depth, this sample contained neither the highest nor the lowest concentration of Zn in base metal sulphides. The two lowermost samples of the Volspruit Sulphide Zone (115.88–116.88 m and 120.88–121.88 m depth) contain the most significant concentrations of As, with up to 219 ppm As in pyrrhotite. Sb only occurs above 1 ppm in pyrrhotite at 106.88–107.88 m depth. The only two elements found to co-vary with depth in the Volspruit Sulphide Zone are Co in pentlandite and Cd in chalcopyrite/cubanite (Fig. 12).

The S/Se values of base metal sulphides from the Volspruit Sulphide Zone are unusually high for magmatic sulphide minerals. Pyrrhotite from the Volspruit Sulphide Zone is characterised by S/Se values ranging from 4,136-21,566. Chalcopyrite and cubanite record S/Se values of 3,377-7,858; S/Se values of 1,405–5,715 were measured in pentlandite. The highest S/Se values occur in pyrrhotite grains from the two lowermost samples of the Volspruit Sulphide Zone (115.88–116.88 m and 120.88–121.88 m depth). These horizons do not contain the greatest concentration of Se-bearing Pb-minerals. In pentlandite and chalcopyrite, increasing S/Se values correspond with a decrease in precious metal concentration. There is poor correlation between S/Se and the tenor of pyrrhotite in samples with S/Se <12,000. However, the analyses with S/Se >12,000 also contain the highest concentration of As (29–219 ppm), Bi (0.2–1.5 ppm) as well as elevated concentrations of Pt (0.1–6 ppm), Ir (0.2–1.6 ppm), Os (0.08–1.1), Ru (1.3–8 ppm), Rh (0.05–30 ppm), Ag (0.2–1 ppm) and Te (bdl-1.2 ppm). These high S/Se samples are notably lower in Re than low S/Se samples. The petrologic setting and texture of these pyrrhotite grains is not visibly different to low S/Se grains. One of the high S/Se values at 115.88–116.88 m occurs adjacent to a Co-rich phase ($\sim Co_3Ni_2Fe_2S_3$). This phase is relatively enriched in As and PGEs with respect to pentlandite, but contains equivalent values of Se, so it cannot be considered a high-Se reservoir. As the magmatic sulphide assemblages were only studied in two dimensions, important accessory phases that we cannot see may affect the trace element budget of individual magmatic sulphide blebs.

4. Discussion

The Volspruit Sulphide Zone is a rare occurrence of sulphide-poor PGE mineralisation in the ultramafic portion of a layered intrusion, with low-grade ore distributed over a ~60 m horizon. It is the only known deposit of this kind in the spectrum of Bushveld PGE mineralisation. Hulbert and von Gruenewaldt (1982, 1985) proposed that the Volspruit Sulphide Zone formed as a consequence of sulphide melt saturation in response to S enrichment in the magma during fractionation. They propose that this ultramafic magma mixed with a sudden influx of denser, cooler and less primitive basaltic magma, which triggered saturation of chromite and sulphides to form the Volspruit Sulphide Zone. In light of the new data presented above, and recent advances in our knowledge of ore-forming processes, we consider that the current genetic models for mineralisation of the Volspruit Sulphide Zone (Hulbert and von Gruenewaldt, 1982, 1985) require significant re-evaluation.

4.1. Evidence to support a high degree of sediment assimilation

We contend that the Volspruit Sulphide Zone experienced a high degree of country rock assimilation. Our interpretation is supported by quantitative geochemical data: (1) high $\delta^{34}S$ values and (2) extremely high S/Se values, further corroborated by qualitative geological observations: (3) local geological relationships, (4) exotic inclusions in chromite, (5) the presence of microxenocrysts and (6) the presence of primary Pb-sulphides, Pb-chlorides and sphalerite in magmatic sulphide assemblages.

4.1.1. Quantitative evidence for assimilation

The Platreef/GNPA orebodies are typically viewed as an end-member for sediment contamination in the Bushveld Complex, as they occur near the contact between the Rustenburg Layered Suite and the country rocks beneath it (granites to the north and interbedded quartzites, shales, limestones and dolomites to the south; Fig. 1b). Sulfur isotopes in the Platreef range from $\delta^{34}S = -0.6$‰ at Zwartfontein (Holwell et al., 2007) to $\delta^{34}S = +10.1$‰ at Townlands (Manyeruke et al., 2005), but are higher than the $\delta^{34}S$ values of the local mantle ($\delta^{34}S = -1.8$ to $+2.4$‰) (Westerlund et al., 2004). Sulfur isotopes of the Volspruit Sulphide Zone ($\delta^{34}S = +3.8$ to $+4.3$‰) are enriched relative to the local mantle (Hulbert, 1983), indicating a significant degree of sedimentary contamination.

Despite the vast literature on sulphide chemistry in the Platreef, the only studies presenting S/Se values of contaminated Platreef/GNPA sulphides are Smith (2014) and Smith et al. (2016). Estimates of S/Se in mantle sulphides (i.e. uncontaminated magmas) range from 2,850–4,350 (Eckstrand and Hulbert, 1987). In mineralised GNPA samples from the Rooipoort area, the highest S/Se values (up to 8,900) occur within secondary pyrite, with S/Se up to 5,600 in primary pyrrhotite (Smith, 2014; Smith et al., 2016). In the Platreef at Turfspruit, the highest S/Se values (up to 10,800) are also recorded in pyrite, with S/Se up to 7,500 in pyrrhotite. Magmatic sulphide assemblages in the Volspruit Sulphide Zone contain the highest S/Se values yet recorded in the Bushveld Complex, with S/Se up to 21,566 in pyrrhotite and 6,804 in chalcopyrite. We return to a more in depth discussion on the origin of extremely high S/Se values after reviewing all the evidence for assimilation in the Volspruit Sulphide Zone.

4.1.2. Qualitative evidence for assimilation

Multiple processes can be invoked to explain the range of $\delta^{34}S$ and S/Se values in the Volspruit Sulphide Zone (c.f. Queffurus and Barnes, 2015; Smith et al., 2016). Fortunately, the regional geology and petrology of samples provide strong, if qualitative evidence in support of sedimentary assimilation, and allow us to identify some of the assimilated sediments.

While ~500 m of the Volspruit subzone is documented beneath the Volspruit Sulphide Zone (Fig. 3), country rock beneath the Volspruit subzone has never been intersected by drilling campaigns. As the lithology and geochemistry of the assimilant(s) is unknown, we are unable to quantify the degree of assimilation using sulfur isotopes or chalcophile trace element modelling. While the proximity of *in situ* country rocks relative to the Volspruit Sulphide Zone remains unknown, one technical mining report implies the presence of metasedimentary xenoliths and their partial melts in the Volspruit Sulphide Zone (EScience Associates (Pty) Ltd, 2011). The map of Hulbert (1983) (Fig. 1c) documents two ~100 m-wide slivers of hornfels, included within the Volspruit subzone, near the northern orebody of the Volspruit Sulphide Zone. These rafts of hornfels appear to be offset by NNW-trending faults, otherwise their relationship to the Volspruit subzone is not documented. The Pretoria Group metasediments are a potential source of contaminants to the Volspruit Sulphide Zone, as they are the closest sedimentary units on a map (Fig. 1c), but the nature of the contact between the Volspruit subzone and Pretoria Group metasediments is unclear. The Pretoria Group metasediments comprise a package of interbedded quartzite and conglomerate, with minor shale/marl and hornfels. At greater depth, beneath the Pretoria Group metasediments, lie the Chuniespoort Group, composed of limestone, dolomite, chert and banded ironstone. Below, we outline why the Chuniespoort Group is a more likely assimilant to the Volspruit Sulphide Zone magmatic system.

Our study has identified the presence of a range of microxenocrysts in the matrix of the Volspruit subzone, microxenocrysts enclosed in chromite as well as enrichments of Pb, Zn and Cl in base metal sulphides, which we attribute to assimilation of country rock. Exotic mineral assemblages enclosed within chromite (e.g. pyroxene +/− plagioclase +/− base metal sulphides accompanied by mica, amphibole,

Table 4
Evaluation of potential assimilants during the formation of the Volspruit Sulphide Zone, based on exotic petrologic assemblages observed in this study.

Petrologic evidence for assimilation in the Volspruit Sulphide Zone	Potential assimilant source(s)				
	Carbonate (limestone/dolomite)	Basinal brines / Pb-Zn mineralisation	Clastic sedimentary	Felsic igneous rocks	Alkaline igneous rocks
Exotic chromite inclusions (Fig. 6 and Fig. 7e)					
Dolomite	✓	✓			
Albite			✓	✓	
Monazite	✓[1]		✓	✓	✓
Pb-Cl	?	✓			
K-Pb-Cl	?	✓			
Microxenocrysts (Fig. 8)					
CaCO₃	✓	✓			
U-Th oxide			✓	✓	✓
Mn-rich ilmenite		✓[2]	✓	✓[3]	✓[4]
Atypical magmatic sulphide assemblages (Fig. 9)					
Sphalerite	?	✓			
Pb-sulphides	?	✓			
Pb-chlorides	?	✓			
K-Pb-Cl	?	✓			

[1] Monazite can form in metasomatic marble (e.g., Deer et al., 1992). [2] Mn-rich ilmenite occurs in stratiform Pb-Zn-Ag ores (e.g., Jiang and Palmer, 1996), as well as granites ([3] e.g., Sasaki et al., 2003), and carbonatites ([4] e.g., Gaspar and Wyllie, 1983).

rutile, quartz, apatite, or zircon) are documented elsewhere in the Bushveld and other layered mafic intrusions, and are attributed to the partial melting and assimilation of country rock (Spandler et al., 2005), mixing with a felsic component (Yao et al., 2017), or the reaction of pyroxene with volatile-rich melts enriched by the introduction of late magmatic fluids expelled during fractional crystallisation (Li et al., 2005). So interpreting a foreign origin for exotic mineral inclusions is not unprecedented. Relative to previous studies (Li et al., 2005; Spandler et al., 2005; Yao et al., 2017; Yudovskaya and Kinnaird, 2010), chromite-hosted mineral inclusions in the Volspruit Sulphide Zone are unusual, because (1) pyroxene is absent and not abundant within silicate inclusions, and (2) relict dolomite is preserved. While post-entrapment equilibration likely alters the distribution of incompatible elements between chromite and included silicate minerals (Spandler et al., 2007), this process cannot explain the exotic mineralogy observed within chromite grains in this study.

In order to assess the end-members for assimilation, we have compiled a list of xenocrystic phases and contaminants, and compared their potential sources (Table 4). While this style of analysis is qualitative, it provides strong evidence in support of carbonate assimilation. The source of albite and U-Th oxide could be from assimilation of a felsic intrusion, or clastic sediments.

The combination of primary Pb-sulphides, Pb-chlorides and sphalerite in base metal sulphide assemblages is rather unusual in magmatic sulphide deposits. It is possible that their presence is under-reported in some studies, because they are (1) accessory minerals, (2) considered as secondary assemblages, and (3) do not concentrate precious metals other than Ag. Sphalerite, galena and Pb-chlorides associated with magmatic sulphides are also documented both Cu-rich ores at Sudbury, Ontario (Dare et al., 2014), and in Cu-Ni ores from the Minnamax deposit, at the base of the Duluth Complex, Minnesota (McSwiggen, 1999). In extreme circumstances (e.g. metamorphosed sulphide deposits), galena and sphalerite can fractionate from a sulphide liquid (Mavrogenes et al., 2013), rather than exsolve from a crystalline sulphide.

The association of primary Pb-sulphides, Pb-chlorides and sphalerite in base metal sulphide assemblages could be explained by either (1) crystallisation from residual liquids, or (2) addition from an external source. While some studies suggest that this mineral assemblage is consistent with a magmatic origin (e.g. Mungall and Brenan, 2003), reviews of sulphide liquid evolution in natural systems (Holwell and McDonald, 2010; Naldrett, 2004) do not include these minerals in the resultant mineral assemblage. As some of the Pb-sulphide inclusions in the Volspruit Sulphide Zone are up to 50 μm across (e.g. the sample at

106.88–107.88 m depth), these accessory minerals should be readily and routinely identified under reflected light if they are typical products of sulphide liquid fractionation.

Instead, the rare association of primary Pb-sulphides, Pb-chlorides and sphalerite within base metal sulphide assemblages imply that Pb, Zn and Cl were added from an external reservoir, and incorporated into the sulphide liquid, as halogens can be dissolved in sulphide melts (c.f. Mungall and Brenan, 2003). Hulbert (1983) notes two localities in Pretoria Group metasediments southeast of the Volspruit orebodies where sulphides are visible (shown with asterisks in Fig. 1c). Unfortunately, no further information on these localities was given. Massive sulphides have been documented in metasedimentary sequences from the Silverton Formation and Timeball Hill Formation, within the Pretoria Group (Reczko et al., 1995). Alternatively, 19 Mississippi Valley-type deposits (enriched in Pb-Zn-F) are documented in the Malmani sub-groups (Chuniespoort Group) and the Campbellrand sub-group – the stratigraphic equivalent of the Malmani subgroup to the west (Martini et al., 1995). These Mississippi Valley-type deposits formed ~2.4–2.35 Ga, after the deposition of the Campbellrand-Malmani dolomite platform ca. 2.55 Ga (Martini et al., 1995). Thus, they were available for assimilation at the time of the Bushveld Complex ca. 2.06 Ga; in fact, some of these Mississippi Valley-type deposits were overprinted by metamorphism associated with the intrusion of the Bushveld Complex (Martini et al., 1995). An alternative hypothesis is that basinal brines (i.e. CO_2-H_2O-Cl ± metal-rich fluids) were introduced to the Volspruit magmatic system at the time of, or prior to chromite mineralisation.

From the range of xenocrysts in Table 4, we infer that assimilation of Mississipi Valley Type deposits hosted within dolomites of the Malmani subgroup is the best explanation for the presence of Pb-chloride minerals in the Volspruit Sulphide Zone. As Mississipi Valley Type deposits are patchy and structurally controlled, there was some serendipity involved creating the Volspruit Sulphide Zone. However, if Pb-chlorides are observed more widely in layered mafic intrusions elsewhere, this interpretation will require revision.

The addition of a Pb and Zn-bearing source did not result in ores with a high proportion of base metal sulphides, as observed in Ni-Cu deposits, where 20–90 vol. % sulphide is typical (Naldrett, 2004). It is possible that assimilation initially created a high volume of sulphide liquid, which was subsequently reduced via sulphide resorbtion (Kerr and Leitch, 2005) or by mechanical sorting during hydrodynamic processes (Maier et al., 2013). In either case, Ni-PGE mineralisation in the Volspruit Sulphide Zone is highly unusual in the spectrum of magmatic

sulphide deposits, as it contains strong evidence for assimilation of sediments yet only contains 2–5 vol. % sulphide.

4.2. Evidence to explain chromite formation

Our study has documented a diverse assemblage of chromite-hosted inclusions (Fig. 6). Hulbert and von Gruenewaldt (1985) observed similar chromite inclusions. They inferred that euhedral, inclusion-free chromite co-crystallised with ultramafic cumulates; *in situ* post-cumulus sintering of chromite produced amoeboidal textures and rounded inclusions (viz. Fig. 6 in Hulbert and von Gruenewaldt, 1985). They attribute the onset of chromite saturation to increased fO_2 caused by fractional crystallisation of mafic minerals. Thus, Hulbert and von Gruenewaldt (1985) consider that chromites are post-cumulus oikocrysts, overgrowing pyroxene chadacrysts from the adjacent assemblage of stratiform cumulates.

The Hulbert and von Gruenewaldt (1985) model – or any model for *in situ* chromite crystallisation (c.f. O'Driscoll et al., 2009) – is not tenable for the Volspruit Sulphide Zone. This is because we observe cumulate assemblages comprised of orthopyroxene and serpentinised mafic silicates, yet a diverse array of mineral inclusions in chromite. Dolomite, sulphides, hydrous and fractionated silicates as well as exotic high-density phases are all present in sub-rounded inclusions. As chromite inclusions are mineralogically distinct from their cumulate matrix (i.e. inclusions are dominated by "exotic" mineralogy rather than pyroxene), we contend that chromite inclusions observed in this study were trapped during chromite crystallisation in an earlier, highly contaminated magma, *prior to emplacement* at the current level in the Volspruit subzone.

The morphology of observed chromite inclusions range from negative crystal shapes to sub-spherical. Inclusions often occur within chains of interconnected chromite clusters, similar to those described in komatiitic cumulates (e.g., Vukmanovic et al., 2013). We envisage that negative crystal shapes and subrounded-rounded inclusions in chromite cores result from dendritic growth and subsequent recrystallisation, as described by Vukmanovic et al. (2013). Dendritic chromite is observed in komatiitic dunites and spinifex zones at or near the flow tops of komatiites, as a result of Cr supersaturation in the melt (e.g., Barnes, 1998).

The diverse mineralogy of chromite-hosted inclusions documented in this study indicate that contamination:

(1) included multiple assimilants (given the mineralogical diversity of the inclusion suite),
(2) introduced felsic and hydrous phases into the magmatic system (e.g. Fig. 6a-d),
(3) introduced carbonate into the magmatic system (Figs. 7e and 8a),
(4) introduced heavy minerals (Pb-chlorides, monazite and U-Th-Pb oxide) into the magma (Fig. 8), and
(5) at certain stages chromite crystallisation was accompanied by sulphide saturation (e.g. Fig. 6e-h).

Chromite saturation (i.e., the limit of Cr solubility) in a melt is controlled by: (1) the initial Cr content, (2) temperature, (3) oxygen fugacity (fO_2), and (4) the activity of SiO_2 (Barnes, 1986, 1998; Murck and Campbell, 1986; Roeder and Reynolds, 1991). While we do not refute Hulbert and von Gruenewaldt (1985)'s observation that chromite assemblages experienced sintering during post-cumulus modification (as evidenced by chains of chromite), we propose that the suite of inclusions in chromite from the Volspruit Sulphide Zone were initially trapped as melt and/or mineral inclusions during rapid onset of chromite crystallisation (i.e. supersaturation of chromite), prior to entering the main Grasvally magma chamber.

4.3. Carbonate assimilation and its affect on oxygen fugacity

Carbonate assimilation is often considered a contributing factor to ore-forming processes in magmatic sulphide deposits (e.g., Harris and Chaumba, 2001; Lehmann et al., 2007; Maier et al., 2007). However, the significance of this contribution is unclear, as there are competing effects of oxidation and reduction during carbonate assimilation and/or following the addition of CO_2 to a magma. To some extent, the assimilation of carbonate will reduce the fO_2 of a melt, because (1) the creation of skarns promote oxidation of Fe, thus reducing the ferric iron content and fO_2 of the magma (Spandler et al., 2012), and (2) increasing the CO_2 content of a melt reduces H_2O solubility, increasing the CO_2/H_2O of the exsolved fluid phase (Mollo et al., 2010). Conversely, the experimental work of Simakin et al. (2012) demonstrates that the addition of CO_2 oxidises Fe in the melt and promotes spinel nucleation. The oxidative capacity of CO_2 addition is also supported by modelling (Wenzel et al., 2002). More recent experiments suggest that carbonate assimilation produces sharp fO_2 gradients within in a magma reservoir (Mollo and Vona, 2014). In natural systems, this process is likely to be rapid (Jolis et al., 2013) and extremely heterogenous, with varied degrees of protolith assimilation (Iacono Marziano et al., 2007) and variation in the composition of the protolith (Ganino et al., 2013), creating temporal fO_2 fluctuations in the magma reservoir. The capacity for CO_2 as an oxidizing or reducing agent also depends on whether a magmatic system is open or closed (Mollo et al., 2010).

In layered intrusions, there is evidence for locally increased fO_2 at the margins of magmatic reservoirs in contact with carbonates. For example, thin chromite stringers are observed between the contact of serpentinized harzburgite and a calc-silicate xenolith in the Lower Chromite zone of the Platreef (Yudovskaya and Kinnaird, 2010). Dolomite xenoliths in the Ioko-Dovyren Intrusion are often mantled by forsterite and spinel rims, and some olivine-spinel skarns contain accessory base metal sulphide assemblages (Wenzel et al., 2002). In this way, it is possible to locally nucleate spinel, base metal sulphide, Mg-rich silicates and Ca-rich pyroxene (e.g. pigeonite), which are diluted during transport from the initial magmatic reservoir.

4.4. How enriched are PGEs in the Volspruit Sulphide Zone?

As platinum-group minerals were directly observed within chromite-hosted sulphide inclusions (Fig. 6), it is unlikely that late-magmatic fluids migrating through the crystal pile (c.f. Boudreau and McCallum, 1992) played a significant role in the PGE enrichment of the Volspruit Sulphide Zone. Instead, the texture and high tenor of base metal sulphides in the Volspruit Sulphide Zone indicate that PGEs were partitioned into an immiscible sulphide liquid, which scavenged PGEs from a larger body of silicate magma (i.e. high R factor).

An inherent problem in reconciling the chalcophile element budget of layered mafic intrusions is that it is difficult to normalise the concentration of elements to 100% sulphide liquid – a calculation necessary for estimating the degree of precious metal enrichment in a sulphide liquid. Recalculating the tenor of base metal sulphides to 100% sulphide in sulphide-poor PGE deposits can create large errors (Barnes and Ripley, 2016). The reasons for this are two-fold: (1) the calculation assumes that chalcophile elements in magmatic sulphide assemblages are only controlled by the minerals pyrrhotite, pentlandite and chalcopyrite, and (2) calculations at such low sulphide concentrations magnify errors. The data in Table 1 is acquired over one-metre drillcore intervals, while the modal abundance of base metal sulphides was variable within each sample and estimated from an area of only a few cm^2. Therefore, these data cannot be reconciled meaningfully. Instead, we use published PGE data with corresponding S analyses from von Gruenewaldt et al. (1989), to estimate the degree of precious metal enrichment required to form the Volspruit Sulphide Zone (i.e., the R factor, where the mass of silicate liquid:sulphide liquid = R:1; Campbell and Naldrett, 1979).
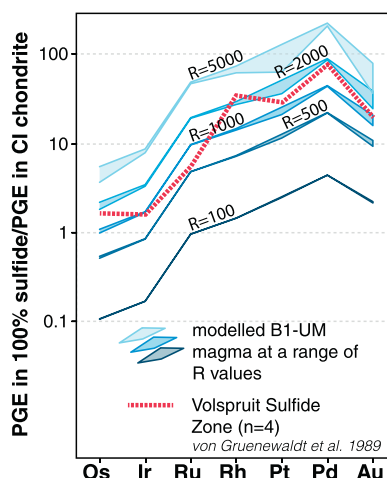
Fig. 13. Estimating the degree of upgrading (R-factor) required to concentrate PGEs in the Volspruit Sulphide Zone from an ultramafic Bushveld magma. The red stippled line shows the measured concentration of PGEs in the Volspruit Sulphide Zone normalised to 100% sulphide and then normalised to CI chondrite (from von Gruenewaldt et al., 1989). The blue outlines show calculated PGE values at a range of sulphide/silicate liquid partition coefficients for given silicate:sulphide mixtures (R-factors) using a B1-UM parental magma (see text for details). This Fig. demonstrates that the mean PGE concentration of the Volspruit Sulphide Zone requires reasonably low silicate:sulphide ratios (500:1 to 3000:1), compared to typical sulphide-poor PGE deposits.

Mineralisation of the Volspruit Sulphide Zone formed from a relatively unfractionated sulphide liquid. Fig. 13 shows the range of R-factors required to concentrate PGEs in the Volspruit Sulphide Zone are between 500:1 to 3000:1, assuming an ultramafic magma (the B1-UM CD-005 magma[9]; Barnes et al., 2010), a range of published partition coefficients (Barnes and Ripley, 2016) and bulk PGE and S analyses from von Gruenewaldt et al. (1989). However, the R-factor may also be controlled by kinetic, rather than equilibrium processes such as the nucleation to growth rate of immiscible sulphide liquid, the rate of chalcophile element diffusion, and the rate of melt migration (Mungall, 2002). In any case, the calculated R factors in the Volspruit Sulphide Zone are orders of magnitude less than R factors from other sulphide-poor PGE deposits. Typically, high-tonnage Ni-Cu sulphide deposits require silicate:sulphide values of 100:1–2000:1, while sulphide-poor PGE deposits such as the Merensky Reef require silicate:sulphide values 10,000:1–100,000:1 (Naldrett, 2004).

The range of Pd measured in pentlandite from the Volspruit Sulphide Zone (39.7–236.4 ppm Pd) is similar to the range of Pd in pentlandite from the GNPA at Rooipoort (below detection-386 ppm Pd; Smith et al., 2014), and the Platreef at Overysel (68.6–183 ppm Pd; Holwell and McDonald, 2007) and Sandsloot (67.7–170 ppm Pd; Holwell and McDonald, 2007). From these data it is evident that PGEs are not homogenously distributed amongst sulphide minerals within a given ore deposit.

4.5. Processes controlling S/Se values in the Volspruit Sulphide Zone

While S/Se values are typically interpreted as direct evidence for contamination of a magma, a range of other processes control them. The first order factors controlling S/Se in magmatic sulphides are (1) S/Se of parent magma mantle values (~3000), (2) prior sulphide saturation events (> S/Se), (3) contamination (S/Se > ~10,000, depending on contaminant) (4) R-factor (< S/Se with > silicate:sulphide and PGE tenor) and (4) crystallisation (S/Se enriched in MSS relative to ISS) (Queffurus and Barnes, 2015). Smith et al. (2016) proposed that

---

[9] The B1-UM chill CD-005 was chosen as ECBV050 (the only other analysis with PGE values) contained less PGEs than the more evolved B1 magma.

sulphide resorbtion (viz. Kerr and Leitch, 2005) lowers the S/Se of the sulphide melt, decoupling proxies for contamination (S/Se and $\delta^{34}S$) in magmatic sulphide assemblages. Secondary alteration from metamorphism, metasomatism from magmatic fluids, and low-temperature processes also preferentially remove S and thus decrease S/Se values (Queffurus and Barnes, 2015).

The first observation about S/Se in the Volspruit Sulphide Zone is that both the $\delta^{34}S$ of bulk sulphide and S/Se of pyrrhotite and chalcopyrite greatly exceed mantle values, providing strong evidence for sediment assimilation. However, we note that the S/Se of Pretoria Group and Chuniespoort Group metasediments likely contain extreme heterogeneity in S/Se. Large et al. (2014) documented rapid fluctuations of Se in marine pyrite around this time period (20–200 ppm) caused by pulses of oxidation preceding the Precambrian great oxidation event, resulting in S/Se values from 2,673 to 26,725 in marine pyrite. Secondly, S/Se values are extremely high compared to the S/Se of Platreef sulphides, confirming low R factors and/or minimal requirement for sulphide resorbtion into the parent magma or secondary alteration in the Volspruit Sulphide Zone. Thirdly, S/Se values in sulphides are not only elevated, but are highly heterogeneous between samples.

Such high S/Se values mean that processes which reduce the S/Se value (R-factor, sulphide resorbtion, S-loss during degassing, metasomatism or alteration) are not a primary control on the S/Se content in the Volspruit Sulphide Zone. Instead, we need to consider processes where sulfur is added, or selenium is lost from base metal sulphides. We think it is unlikely that S-addition from assimilation alone can account for the high S/Se values, for two reasons. Firstly, some of the S/Se values recorded in this study are greater than postulated sedimentary end-members. For example, sedimentary rocks with the highest S/Se are sulphide-bearing sediments, such as black shales (Queffurus and Barnes, 2015), yet we have noted that pyrite in marine shales beneath the Volspruit subzone should be characterised by S/Se of 2,673-26,725. So to create pyrrhotite where S/Se = 21,566 would require an implausibly high degree of mixing. Unfortunately, Se has not been measured in the country rocks beneath the Bushveld Complex. Secondly, if S-addition from assimilation were the primary control on S/Se, then this should dilute the tenor of the sulphide minerals. That is, we would expect to see PGE grade of sulphides decrease with S/Se, which we do not observe in pyrrhotite (Fig. 14).

So while we consider that S-addition is an important control on S/Se in the Volspruit Sulphide Zone (evidenced by the addition of Pb and Zn into base metal sulphides), another process must be invoked to explain the high and heterogenous S/Se values. Exploring processes whereby Se is lost from sulphide is the only remaining option.

Initially, we considered that the high and heterogenous S/Se values may be caused by precipitation of Se-bearingPb-sulphides and Se-bearing Pb-chlorides from a fractionating sulphide melt. Se is known to be highly compatible in the structure of galena, along with Ag and other semi-metals such as Te and Bi (George et al., 2015, 2016). Thus, we can test the influence of galena and Pb-chlorides on the S/Se of sulphides during sulphide melt evolution by assessing the depletion of Ag, Te and Bi with S/Se values (Fig. 14). If the high S/Se of pyrrhotite is inherited from fractionation of galena (i.e. Se removal) from a sulphide melt– noting that galena may not necessarily be visible in the exposed, polished sulphide bleb – then high S/Se analyses should correlate with the lowest values of Ag, Te and Bi, elements also highly compatible in galena. However, this is not observed in pyrrhotite (Fig. 14), indicating that high S/Se in pyrrhotite is not inherited from fractionation of galena. Ag decreases with increasing S/Se in chalcopyrite, but not Te and Bi. It is more likely that Ag varies with Au and PGEs, rather than being controlled by the S/Se (and thus galena fractionation) in chalcopyrite. These data are also supported by the observation that Se-bearing Pb-chlorides or Pb-sulphides were not observed at 115.88–116.88 m and 120.88–121.88 m depth, where the greatest S/Se values are recorded.
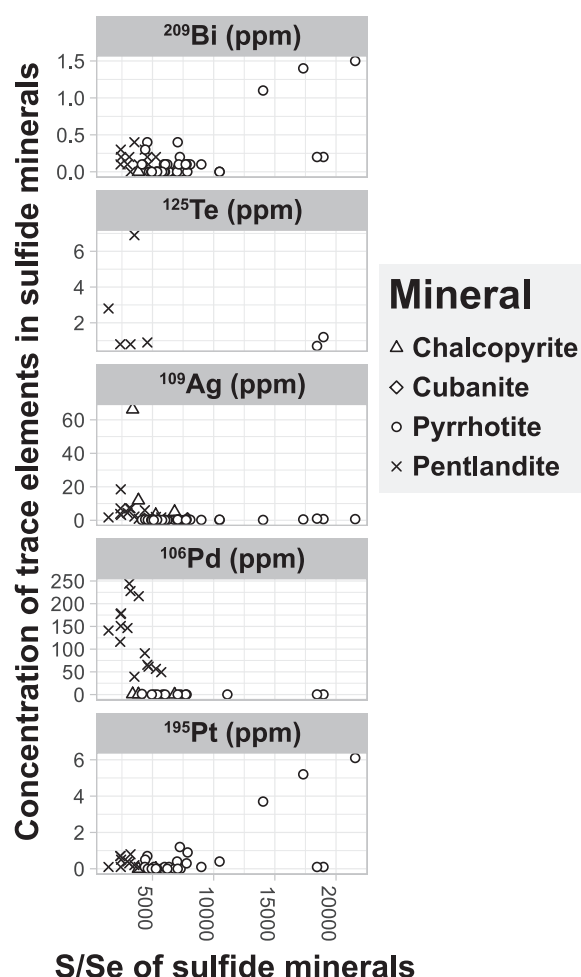
Fig. 14. Selected trace elements plotted against S/Se for the four different minerals analysed in this study, to interrogate the origin of high S/Se values. As the PGE grade of pyrrhotite does not decrease with increasing S/Se, S-addition alone cannot explain the high S/Se values in pyrrhotite. If high S/Se is inherited from the fractionation of Se-bearing galena from a magmatic sulphide melt, then we would expect Ag, Te and Ag to decrease in other base metal sulphides with increasing S/Se, which is not observed.

degassing in magmatic systems e.g., (Jenner et al., 2010). Fig. 10 in Jenner et al. (2010) suggests the transition from immobile selenite to volatile selenate may begin above ~FMQ + 2. Regardless of the absolute values of the selenite-selenate transition, it is likely that assimilating carbonate country rocks into an ultramafic magma will produce extreme gradients in fO_2. Locally, portions of magma in close contact with country rock may become extremely oxidised, accompanied by extensive degassing from surrounding carbonates. In such an environment, we consider that it might be possible to oxidise Se to a volatile selenate species – so that *both* S and Se would be lost during degassing. Small changes in the oxidation state could change the proportion of Se lost. Thus, assimilation of a sulphide-rich carbonate would alter the S/Se of magmas in the Volspruit subzone by adding crustal S, and by local removal of S and Se via degassing of an oxidised magma. We consider this process the best available explanation to explain high and heterogenous S/Se values in the Volspruit Sulphide Zone.

An alternative hypothesis to explain the high S/Se values is that Se was removed from sulphides in the Volspruit Sulphide Zone during oxidation by high-pH postmagmatic fluids, as observed in the Jinchuan Ni-Cu-PGE deposit (Prichard et al., 2013). However, this hypothesis is not supported by either (1) the range of Se concentrations observed in sulphides, or (2) the absence of an alteration overprint in BMS assemblages. As pentlandite contains up to 237 ppm Se, this hypothesis would require Se to be selectively leached from pyrrhotite, but retained in pentlandite. As Se is less mobile than S (Prichard et al., 2013), postmagmatic alteration of BMS should create secondary mineral assemblages. For example, alteration with no sulfur loss would create an assemblage of millerite, magnetite, pyrite, violarite and/or cubanite, or abundant magnetite with rare millerite, violarite or cubanite if sulfur is lost from the system (e.g. Holwell et al., 2017; Prichard et al., 2013; Ripley et al., 2005; Smith et al., 2016). These secondary mineral assemblages were not observed in the Volspruit Sulphide Zone.

Therefore, we think the data in this study best supports the model for S-addition and subsequent Se- and S-degassing during assimilation as an explanation for the high S/Se values.

4.6. Origin of the Volspruit Sulphide Zone

Here, we summarise the paragenetic sequence of events leading to the creation of the Volspruit Sulphide Zone (Fig. 15).

4.6.1. Source magma

Cumulates from the Volspruit subzone cannot have formed from a B1 magma under reasonable conditions (Yudovskaya et al., 2013), as they contain relatively unevolved compositions: up to 47.52 wt% Cr_2O_3 in chromite, up to En_{90} in orthopyroxene and up to Fo_{90} in olivine. Yudovskaya et al. (2013) propose that chills from the Basal Ultramafic Sequence (Wilson, 2015), or analyses of B1-UM chills CD-005 and ECBV050 (Barnes et al., 2010) would be suitable candidates for parental magmas. Of these, PGE analyses of the B1-UM chills CD-005 are most appropriate. Contrary to Hulbert and von Gruenewaldt's (1982) model, we found no evidence to support the contribution of a more evolved B1, B2, or B3 magma (Barnes et al., 2010), a "denser, cooler and less primitive basaltic liquid" (pp. 306, Hulbert, 1983), or northern limb Main Zone-style magma (McDonald et al., 2005).

Given the Pt/Pd of suitable parental magmas is 1.08–2.13 (Barnes et al., 2010), while the Pt/Pd of the modelled PGE resources in the northern limb are consistently <1.0 (Table 1), it is likely that the Lower Zone of the northern limb had a separate ultramafic source with distinct highly siderophile element chemistry from magmas in the eastern limb of the Bushveld Complex. While the B1 magma contains 33 ppb Pt + Pd, the ultramafic chill B1-UM CD-005 contains 50 ppb Pt + Pd (Barnes et al., 2010). Therefore, less upgrading is required to form a viable ore deposit.

In order to fully exclude this hypothesis, we calculated the influence of accessory Se-bearing sulphides (galena and Pb-chlorides) on the S/Se budget of the sulphide liquid. While petrologically significant, the volume of Pb-sulphide and Pb chlorides in the Volspruit is extremely small. Of the 33 cm² searched for high-density minerals in this study, Pb sulphides account for 0.0002 area % and Pb-chlorides account for 0.00002 area %. So assuming mean modal proportions of base metal sulphides from Hulbert (1983) and normalising these to 3 area %, we considered the effect of adding or removing the mean proportion of galena and Pb-chloride measured in this study, assuming a very generous estimate of 2 wt% Se in each Pb-phase. As these phases are volumetrically insignificant, they only increased the S/Se of the sulphide liquid by 0.01%. Thus, at such a low volume, crystallisation of Se-rich Pb-sulphides and Pb-chlorides is unlikely to control the S/Se budget of individual magmatic sulphide blebs.

Secondly, we considered the possibility that Se is lost during degassing. In basaltic systems, the proportion of sulfate in a melt ($S^{6+}/\Sigma S$) increases above ~FMQ-1 e.g., Jugo et al. (2005). So above ~FMQ-1, sulfur becomes increasingly volatile and may be lost during degassing. While the speciation of $Se^{6+}/\Sigma Se$ with oxidation state in basaltic systems is not defined, the transition from immobile selenide to volatile selenate is estimated to occur at much higher oxidation states. This is why S/Se is used as a proxy for

4.6.2. Magma intruded assimilant(s) beneath the Rustenburg Layered Suite

We observed sulphide inclusions, silicate inclusions and trapped crustal assimilants within chromite. As these inclusions typically occur in the centre of chromite grains, we infer that inclusions were trapped soon after chromite crystals nucleated in the parent magma. Thus, these trapped inclusions record the earliest magmatic processes during the formation of the Volspruit Sulphide Zone. As these chromite inclusions (1) occur in the centre of chromite grains, (2) do not match the composition of minerals typically observed in the Volspruit subzone, and (3) contain dolomite, albite, hydrous phases, monazite and Pb-chlorides – we consider that these inclusions record the earliest history of magmatic emplacement into sedimentary rocks in a staging chamber/sill beneath the main Grasvally magma chamber (i.e. beneath the Rustenburg Layered Suite).

We envisage that primitive, ultramafic magmas intruded along a sedimentary contact beneath the main Grasvally magma chamber. The record of assimilation from microxenocrysts (e.g., calcium carbonate, U-Th oxide, Mn-rich ilmenite), exotic chromite inclusions (e.g., dolomite, albite, monazite) and Pb and Zn-rich magmatic sulphide assemblages indicate that limestone and dolomite were assimilated along at least one margin of this contact. The most voluminous local source of calcite and dolomite is the Malmani dolomite, which is also a documented host of Pb-Zn Mississippi Valley-type deposits (Martini

et al., 1995). As the Malmani dolomite rests above the Black Reef Quartzite, we postulate that this contact may be the location of the sub-Grasvally staging chamber.

4.6.3. Assimilation of oxidised sediments triggered chromite saturation

Assimilation of carbonates with a minor contribution from other sediments locally increased the fO_2 of the ultramafic magma and triggered chromite saturation, evidenced by the presence of the exotic chromite inclusions. Assimilation of carbonates may be accompanied by extensive volatilisation of CO_2, released from assimilants and adjacent country rock, creating a turbulent magmatic environment. Despite a potentially turbulent environment, the heterogeneity of assimilants in the magma could still create sharp gradients in fO_2, and thus fronts of chromite crystallisation in the magma.

4.6.4. Chromite crystallisation and addition of external sulfur triggered sulphide saturation

As sulphide inclusions are not consistently observed in chromites, we propose that chromite saturation preceded sulphide saturation, but there was at least one period where both processes were simultaneous. It is likely that saturation of an immiscible sulphide liquid was triggered by (1) addition of external sulfur from sedimentary contaminants, and (2) a decrease in Fe following chromite crystallisation
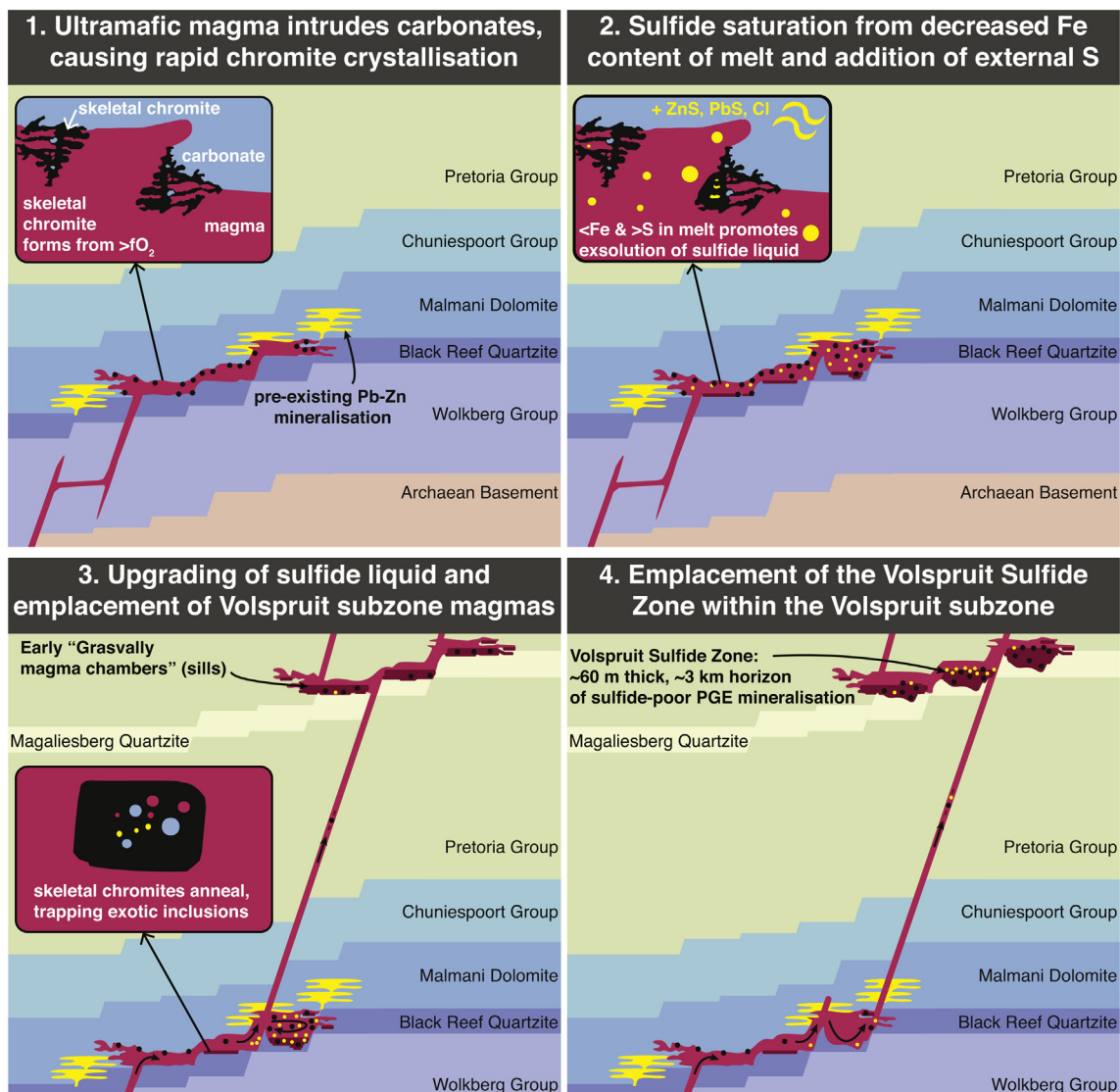

Fig. 15. Schematic diagram outlining our revised model for ore genesis in the Volspruit Sulphide Zone.

(lowering the amount of sulfur required to achieve sulphide saturation). It is possible that sulphide saturation was triggered by a sudden influx of sedimentary sulfur, such as assimilating pre-existing Pb-Zn Mississippi Valley-type mineralisation, basinal brines, or a large quantity of sedimentary sulfur. Continued carbonate assimilation would create sharp fO_2 gradients surrounding large xenoliths and roof pendants, accompanied by degassing of S and probably Se. During this process, remaining immiscible sulphide liquid would be stirred amongst silicate liquid, at a ratio of <3000:1. Periods of quiescence with less assimilation and magma replenishment would allow cumulates to settle, forming chains of chromite and sintered chromite textures.

4.6.5. Emplacement of crystal-rich slurries into the main Grasvally magma chamber

A turbulent pulse of magma or a sudden fault rupture moves crystal-rich slurries containing entrained sulphide droplets, chromite crystals and pyroxene grains out of the staging chamber and into the growing Volspruit subzone in the main Grasvally magma chamber. The chromite-sulphide-silicate slurry is emplaced as a stratiform horizon – the full extent of this layer remains unknown – it is unlikely to be as contiguous as the Merensky Reef. We estimate that the Volspruit Sulphide Zone is restricted to a Grasvally sub-chamber ~60 m thick and continuous ~3 km along strike (Fig. 1C). During and following this event, emplacement of the Volspruit subzone continues.

4.6.6. Crystallisation of the Volspruit Sulphide Zone

There is very little plagioclase present in the Volspruit subzone, so the volume of trapped intercumulus melt is very small. Most of the interstitial liquid must have been squeezed out from the weight of overlying cumulates, and mixed with magmas above it. As the cumulates cooled, interstitial sulphide melt droplets fractionated, exsolving a copper-rich liquid, crystallising Fe-Ni-rich monosulphide solution and Cu-rich intermediate solid solution, before crystallising the observed base metal sulphide and precious metal mineral assemblages (e.g. Holwell and McDonald, 2010; Naldrett, 2004).

4.6.7. Post-cumulus serpentinisation of Volspruit subzone – fluid flow during reheating?

The metamorphic aureole surrounding the northern limb of the Bushveld Complex records two stages of contact metamorphism. These are attributed to (1) emplacement of the Lower Zone and (2) emplacement of layered rocks above Lower Zone cumulates (Nell, 1985). McDonald et al. (2005) contend that emplacement of the GNPA and overlying magmatic stratigraphy occurred while there was still melt replenishment occuring in the Grasvally (Lower Zone) magma chamber, but replenishment of Lower Zone magmas north of Grasvally had ceased. However van der Merwe (2008)) assert that there was a major hiatus between emplacement of Lower Zone and Main Zone magmas. The data from this study can neither confirm nor deny these hypotheses.

If van der Merwe (2008)'s hypothesis is correct, alteration and serpentinisation of the Volspruit deposit could have occurred during the emplacement of overlying magmas. However, it is most likely that alteration and serpentinisation of the Volspruit cumulates occurred during low-grade regional metamorphism associated with gentle folding and/or one of the four episodes of faulting recorded in the region (Hulbert, 1983; van der Merwe, 2008). We postulate that the regional metamorphism must have been low grade, as we observed no evidence for melting and remobilisation of sulphides. However, it is difficult to provide evidence for remelting of magmatic sulphide assemblages, as magmatic assemblages are texturally similar. Serpentinisation affected base metal sulphides more or less equally – precious metal minerals are the only phases that are not altered.

4.7. Would we expect another Volspruit-style deposit in the Bushveld Complex?

To date, there are no other ore deposits in the Bushveld Complex similar to the Volspruit Sulphide Zone, implying that these ore-forming processes are unique. We propose that assimilation of a carbonate unit containing significant sulfur and subsequent crystallisation of chromite was crucial to the formation of an immiscible sulphide liquid in the initial sulphide-undersaturated ultramafic magma. The presence of Pb-sulphides, Pb-chlorides and sphalerite suggests that this magma may have assimilated pre-existing Pb-Zn mineralisation or basinal brines. We consider that the Malmani Dolomite is the most likely assimilant. As the Malmani Dolomite extends across the Kaapvaal craton, it is possible that other staging chambers could have assimilated this horizon, but the resulting mineralisation in the main Bushveld chamber is likely to be localised and not continuous across great distances.

It is possible that the occurrence of even sub-economic Volspruit-style mineralisation in ultramafic cumulates could reduce the grade and opportunity for PGE mineralisation events higher up in the local magmatic stratigraphy of a layered intrusion (c.f., Latypov et al., 2017), or in or in subsequent magma emplacement events sourced from the same reservoir (c.f., Mungall et al., 2016). However, given the low R-factors required to form Volspruit-style mineralisation, the presence of this type of mineralisation does not necessarily preclude further opportunities for creating economically viable concentrations of PGEs.

5. Conclusion

This study demonstrates that qualitative petrological evidence such as detailed inclusion and microxenocryst studies provide additional lines of evidence for assimilation, complementing existing quantitative geochemical proxies such as the S/Se ratio and sulfur isotope compositions. Identification of microxenocrysts is particularly useful when the end-member compositions of assimilants is not known. These new qualitative techniques could be applied beyond layered intrusion research, to identify the range of crustal contaminants in other magmatic systems where macro-xenoliths are neither sampled nor preserved.

We consider that the Volspruit Sulphide Zone formed as a result of the following processes:

1. Parental magmas are derived from a fertile ultramafic source, similar to B1-UM in composition.
2. The ultramafic source intruded into carbonate sediments (possibly the contact between the Malmani dolomite and the Black Reef quartzite) beneath the main Grasvally chamber in the northern Bushveld Complex.
3. Assimilated carbonate rocks increased the fO_2 of the ultramafic magma, triggering rapid precipitation of chromite.
4. Addition of external sulfur from the sedimentary assimilant, coupled with the sudden reduction in the Fe content of the melt from chromite crystallisation triggered the exsolution of an immiscible sulphide phase. It is possible that addition of external sulfur, Pb, Zn and Cl was enhanced by the assimilation of pre-existing Pb-Zn-Cl mineralisation or basinal brines.
5. Chromite, base metal sulphides and pyroxene were emplaced into the Grasvally chamber as a crystal-bearing slurry, forming a PGE horizon ~ 60 m thick and ~ 3 km wide.
6. The ~60 m thick Volspruit Sulphide Zone crystallised and underwent post-cumulus serpentinisation that did not alter PGE distribution.

While mineralisation in the ultramafic portions of layered intrusions is uncommon, it is possible for PGE mineralisation to occur in these environments if the ultramafic magmas intrude in the vicinity of carbonate sediments. It is possible that Volspruit-style mineralisation may reduce the opportunity for economically viable PGE mineralisation higher up in

the local magmatic stratigraphy of a layered intrusion, or in later magma emplacement events sourced from the same reservoir.

Acknowledgements

Appendix A. Supplementary data

Supplementary data to this article can be found online at https://doi.org/10.1016/j.lithos.2018.10.032.

References

Barnes, S.J., 1986. The distribution of chromium among orthopyroxene, spinel and silicate liquid at atmospheric pressure. Geochim. Cosmochim. Acta 50, 1889–1909. doi: https://doi.org/10.1016/0016-7037(86)90246-2

Barnes, S.J., 1998. Chromite in komatiites, 1. Magmatic controls on crystallization and composition. J. Petrol. 39, 1689–1720. doi:https://doi.org/10.1093/petroj/39.10.1689

Barnes, S.J., Ripley, E.M., 2016. Highly siderophile and strongly chalcophile elements in magmatic ore deposits. Rev. Mineral. Geochem. 81, 725–774. https://doi.org/10.2138/rmg.2016.81.12.

Barnes, S.J., Anderson, J.A.C., Smith, T.R., Bagas, L., 2008. The Mordor Alkaline Igneous Complex, central Australia: PGE-enriched disseminated sulphide layers in cumulates from a lamprophyric magma. Mineral. Deposita 43, 641–662. https://doi.org/10.1007/s00126-008-0187-1.

Barnes, S.J., Maier, W.D., Curl, E.A., 2010. Composition of the marginal rocks and sills of the Rustenburg Layered Suite, Bushveld Complex, South Africa: Implications for the formation of the platinum-group element deposits. Econ. Geol. 105, 1491–1511. https://doi.org/10.2113/econgeo.105.8.1491.

Barnes, S.J., Osborne, G.A., Cook, D., Barnes, L., Maier, W.D., Godel, B., 2011. The Santa Rita nickel sulphide deposit in the Fazenda Mirabela Intrusion, Bahia, Brazil: Geology, sulphide geochemistry, and genesis. Econ. Geol. 106, 1083–1110. https://doi.org/10.2113/econgeo.106.7.1083.

Barnes, S.J., Mungall, J.E., Le Vaillant, M., Godel, B., Lesher, C.M., Holwell, D.A., Lightfoot, P.C., Krivolutskaya, N., Wei, B., 2017. Sulphide-silicate textures in magmatic Ni-Cu-PGE sulphide ore deposits : Disseminated and net-textured ores. Am. Mineral. 102, 473–506.

Boudreau, A.E., McCallum, I.S., 1992. Concentration of platinum-group elements by magmatic fluids in layered intrusions. Econ. Geol. 87, 1830–1848. https://doi.org/10.2113/gsecongeo.87.7.1830.

Cameron, E.N., 1978. The Lower Zone of the eastern Bushveld Complex in the Olifants River Trough. J. Petrol. 19, 437–462. https://doi.org/10.1093/petrology/19.3.437.

Campbell, I., Naldrett, A.J., 1979. The influence of silicate-sulphide ratios on the geochemistry of magmatic sulphides. Econ. Geol. 74, 1503–1506. https://doi.org/10.2113/gsecongeo.74.6.1503.

Cawthorn, R.G., 2015. The Bushveld Complex, South Africa. In: Charlier, B., Namur, O., Latypov, R., Tegner, C. (Eds.), Layered Intrusions. Springer, pp. 517–588.

Chaumba, J., 2017. Hydrothermal alteration in the Main Sulphide Zone at Unki Mine, Shurugwi Subchamber of the Great Dyke, Zimbabwe: Evidence from petrography and silicate mineral chemistry. Minerals 7. , pp. 127, 1–41 https://doi.org/10.3390/min7070127.

Dare, S.A.S., Barnes, S.J., Prichard, H.M., Fisher, P.C., 2014. Mineralogy and geochemistry of Cu-rich ores from the McCreedy east Ni-Cu-PGE deposit (Sudbury, Canada): Implications for the behavior of platinum group and chalcophile elements at the end of crystallization of a sulphide liquid. Econ. Geol. 109, 343–366. https://doi.org/10.2113/econgeo.109.2.343.

Deer, W.A., Howie, R.A., Zussman, J., 1992. An Introduction to the Rock-forming Minerals. Second edition. Longman Scientific & Technical, New York, Wiley.

van der Merwe, F., 1976. The layered sequence of the Potgietersrus Limb of the Bushveld Complex. Econ. Geol. 71, 1337–1351.

van der Merwe, M.J., 2008. The geology and structure of the Rustenburg Layered Suite in the Potgietersrus/Mokopane area of the Bushveld Complex, South Africa. Miner. Depos. 43, 405–419. https://doi.org/10.1007/s00126-007-0168-9.

Diella, V., Ferrario, A., Girardi, V.A.V., 1995. PGE and PGM in the Luanga mafic-ultramafic intrusion in Serra dos Carajás (Pará State, Brazil). Ore Geol. Rev. 9, 445–453. https://doi.org/10.1016/0169-1368(95)00002-J.

Eales, H.V., Cawthorn, R.G., 1996. The Bushveld Complex. Dev. Petrol. 15, 181–229. https://doi.org/10.1016/S0167-2894(96)80008-X.

Eckstrand, O.R., Hulbert, L.J., 1987. Selenium and the source of sulfur in magmatic nickel and platinum deposits. Geological Association of Canada–Mineralogical Association Canada Program with Abstracts, p. 40.

EScience Associates (Pty) Ltd, 2011. Final Scoping Report: Proposed Establishment of an open-cast PGM Mine on the Farm Volspruit 326 KR and the Farm Zoetveld 294 KR, Mokopane District, Limpopo Province.

Ganino, C., Harris, C., Arndt, N.T., Prevec, S.A., Howarth, G.H., 2013. Assimilation of carbonate country rock by the parent magma of the Panzhihua Fe-Ti-V deposit (SW China): Evidence from stable isotopes. Geosci. Front. 4, 547–554. https://doi.org/10.1016/j.gsf.2012.12.006.

Gaspar, J.C., Wyllie, P.J., 1983. Ilmenite (high Mg, Mn, Nb) in the carbonatites from the Jacupiranga complex, Brazil. Am. Mineral. 68, 960–971.

George, L.L., Cook, N.J., Ciobanu, C.L., Wade, B.P., 2015. Trace and minor elements in galena: A reconnaissance LA-ICP-MS study. Am. Mineral. 100, 548–569.

George, L.L., Cook, N.J., Ciobanu, C.L., 2016. Partitioning of trace elements in co-crystallized sphalerite-galena-chalcopyrite hydrothermal ores. Ore Geol. Rev. 77, 97–116. https://doi.org/10.1016/j.oregeorev.2016.02.009.

Gervilla, F., Kojonen, K., 2002. The platinum-group minerals in the Upper Section of the Keivitsansarvi Ni-Cu-PGE Deposit, Northern Finland. Can. Mineral. 40, 377–394. https://doi.org/10.2113/gscanmin.40.2.377.

Grokhovskaya, T.L., Ivanchenko, V.N., Karimova, O.V., Griboedova, I.G., Samoshnikova, L.A., 2012. Geology, mineralogy, and genesis of PGE mineralization in the South Sopcha massif, Monchegorsk complex, Russia. Geol. Ore Depos. 54, 347–369. https://doi.org/10.1134/S1075701512050029.

von Gruenewaldt, G., Walraven, F., 1980. Bushveld Complex. In: The South African Committee for Stratigraphy (Ed.), Stratigraphy of South Africa, Handbook 8, Part 1: Lithostratigraphy of the Republic of South Africa, South West Africa/Namibia and the Republics of Bophuthatswana. Transkei and Venda. Republic of South Africa Geological Survey, pp. 223–242.

von Gruenewaldt, G., Hulbert, L.J., Naldrett, A.J., 1989. Contrasting platinum-group element concentration patterns in cumulates of the Bushveld complex. Mineral. Deposita 24, 219–229. https://doi.org/10.1007/BF00206445.

Harris, C., Chaumba, J.B., 2001. Crustal contamination and fluid–rock interaction during the formation of the Platreef, northern limb of the Bushveld Complex, South Africa. J. Petrol. 42, 1321–1347. https://doi.org/10.1093/petrology/42.7.1321.

Helmy, H.M., Mogessie, A., 2001. Gabbro Akarem, Eastern Desert, Egypt: Cu-Ni-PGE mineralization in a concentrically zoned mafic-ultramafic complex. Mineral. Deposita 36, 58–71. https://doi.org/10.1007/s001260050286.

Holwell, D.A., McDonald, I., 2007. Distribution of platinum-group elements in the Platreef at Overysel, northern Bushveld Complex: A combined PGM and LA-ICP-MS study. Contrib. Mineral. Petrol. 154, 171–190. https://doi.org/10.1007/s00410-007-0185-9.

Holwell, D.A., McDonald, I., 2010. A review of the behaviour of platinum group elements within natural magmatic sulphide ore systems. Platin. Met. Rev. 54, 26–36. https://doi.org/10.1595/147106709X480913.

Holwell, D.A., Boyce, A.J., McDonald, I., 2007. Sulfur isotope variations within the Platreef Ni-Cu-PGE deposit: Genetic implications for the origin of sulphide mineralization. Econ. Geol. 102, 1091–1110. https://doi.org/10.2113/gsecongeo.102.6.1091.

Holwell, D.A., Adeyemi, Z., Ward, L.A., Smith, D.J., Graham, S.D., McDonald, I., Smith, J.W., 2017. Low temperature alteration of magmatic Ni-Cu-PGE sulphides as a source for hydrothermal Ni and PGE ores: A quantitative approach using automated mineralogy. Ore Geol. Rev. 91, 718–740. doi:https://doi.org/10.1016/j.oregeorev.2017.08.025

Hulbert, L.J., 1983. A Petrological Investigation of the Rustenburg Layered Suite and Associated Mineralization South of Potgietersrus. D.Sc. thesis. University of Pretoria.

Hulbert, L.J., von Gruenewaldt, G., 1982. Nickel, copper, and platinum mineralization in the lower zone of the Bushveld Complex , South of Potgietersrus. Econ. Geol. 77, 1296–1306.

Hulbert, L.J., von Gruenewaldt, G., 1985. Textural and compositional features of chromite in the Lower and Critical Zones of the Bushveld Complex south of Potgietersrus. Econ. Geol. 80, 872–895. https://doi.org/10.2113/gsecongeo.80.4.872.

Hunter, R.H., 1996. Texture Development in Cumulate Rocks. Dev. Petrol. 15, 77–101. https://doi.org/10.1016/S0167-2894(96)80005-4.

Huthmann, F.M., Yudovskaya, M.A., Kinnaird, J.A., Mccreesh, M., McDonald, I., 2018. Geochemistry and PGE of the lower mineralized Zone of the Waterberg Project, South Africa. Ore Geol. Rev. 92, 161–185. https://doi.org/10.1016/j.oregeorev.2017.10.023.

Iacono Marziano, G., Gaillard, F., Pichavant, M., 2007. Limestone assimilation and the origin of CO_2 emissions at the Alban Hills (Central Italy): Constraints from experimental petrology. J. Volcanol. Geotherm. Res. 166, 91–105. https://doi.org/10.1016/j.jvolgeores.2007.07.001.

Irvine, T.N., 1980. Magmatic density currents and cumulus processes. Am. J. Sci. 280, 1–58.

Jenner, F.E., O'Neill, H.S.C., Arculus, R.J., Mavrogenes, J.A., 2010. The magnetite crisis in the evolution of arc-related magmas and the initial concentration of Au, Ag and Cu. J. Petrol. 51, 2445–2464. https://doi.org/10.1093/petrology/egq063.

Jiang, S.-Y., Palmer, M.R., 1996. Mn-rich ilmenite from the sullivan Pb-Zn-Ag deposit, British Columbia. Can. Mineral. 34, 29–36.

Jolis, E.M., Freda, C., Troll, V.R., Deegan, F.M., Blythe, L.S., McLeod, C.L., Davidson, J.P., 2013. Experimental simulation of magma-carbonate interaction beneath Mt. Vesuvius, Italy. Contrib. Mineral. Petrol. 166, 1335–1353. https://doi.org/10.1007/s00410-013-0931-0.

Joubert, P., Johnson, M.R., 1998. Abridged lexicon of South African stratigraphy. Council for Geoscience.

Jugo, P.J., Luth, R.W., Richards, J., 2005. Experimental data on the speciation of sulfur as a function of oxygen fugacity in basaltic melts. Geochim. Cosmochim. Acta 69, 497–503. https://doi.org/10.1016/j.gca.2004.07.011.

Kaavera, J., Rajesh, H.M., Tsunogae, T., Belyanin, G.A., 2018. Marginal facies and compositional equivalents of Bushveld parental sills from the Molopo Farms Complex layered intrusion, Botswana: Petrogenetic and mineralization implications. Ore Geol. Rev. 92, 506–528. https://doi.org/10.1016/j.oregeorev.2017.12.001.

Karykowski, B.T., 2017. New Approaches in Understanding Layered Intrusions: Field-Based and Analytical Evidence From the Bushveld and Monchegorsk Complexes. Ph.D. thesis. Cardiff University.

Karykowski, B.T., Maier, W.D., Groshev, N.Y., Barnes, S.J., Pripachkin, P.V., McDonald, I., Savard, D., 2018. Critical controls on the formation of contact-style PGE-Ni-Cu mineralization: Evidence from the Paleoproterozoic Monchegorsk Complex, Kola Region, Russia. Econ. Geol. 113, 911–935. https://doi.org/10.5382/econgeo.2018.4576.

Kerr, A., Leitch, A.M., 2005. Self-destructive sulphide segregation systems and the formation of high-grade magmatic ore deposits. Econ. Geol. 100, 311–332. https://doi.org/10.2113/gsecongeo.100.2.311.

Kinnaird, J.A., McDonald, I., 2005. An introduction to mineralisation in the northern limb of the Bushveld Complex. Appl. Earth Sci. 114, 194–198. https://doi.org/10.1179/037174505X62893.

Kinnaird, J.A., Yudovskaya, M., McCreesh, M., Huthmann, F., Botha, T.J., 2017. The Waterberg platinum group element deposit: Atypical mineralization in mafic-ultramafic rocks of the Bushveld Complex, South Africa. Econ. Geol. 112, 1367–1394. https://doi.org/10.5382/econgeo.2017.4513.

Knight, R.D., Prichard, H.M., McDonald, I., Ferreira Filho, C.F., 2011. Platinum-group mineralogy of the Fazenda Mirabela intrusion, Brazil: the role of high temperature liquids and sulphur loss. Appl. Earth Sci. 120, 211–224. https://doi.org/10.1179/1743275812Y.0000000016.

Large, R.R., Halpin, J.A., Danyushevsky, L.V., Maslennikov, V.V., Bull, S.W., Long, J.A., Gregory, D.D., Lounejeva, E., Lyons, T.W., Sack, P.J., McGoldrick, P.J., Calver, C.R., 2014. Trace element content of sedimentary pyrite as a new proxy for deep-time ocean-atmosphere evolution. Earth Planet. Sci. Lett. 389, 209–220. https://doi.org/10.1016/j.epsl.2013.12.020.

Latypov, R.M., Chistyakova, S., Kramers, J.D., 2017. Arguments against syn-magmatic sills in the Bushveld Complex, South Africa. South African J. Geol. 120 (4), 565–574. https://doi.org/10.25131/gssajg.120.4.565.

Le Bas, M.J., Streckeisen, A.L., 1991. The IUGS systematics of igneous rocks. J. Geol. Soc. Lond. 148, 825–833. https://doi.org/10.1144/gsjgs.148.5.0825.

Le Vaillant, M., Barnes, S.J., Fiorentini, M.L., Santaguida, F., Törmänen, T., 2016. Effects of hydrous alteration on the distribution of base metals and platinum group elements within the Kevitsa magmatic nickel sulphide deposit. Ore Geol. Rev. 72, 128–148. https://doi.org/10.1016/j.oregeorev.2015.06.002.

Lehmann, J., Arndt, N., Windley, B., Zhou, M.F., Wang, C.Y., Harris, C., 2007. Field relationships and geochemical constraints on the emplacement of the Jinchuan intrusion and its Ni-Cu-PGE sulphide deposit, Gansu. China. Econ. Geol. 102, 75–94. https://doi.org/10.2113/gsecongeo.102.1.75.

Li, C., Ripley, E.M., Sarkar, A., Shin, D., Maier, W.D., 2005. Origin of phlogopite-orthopyroxene inclusions in chromites from the Merensky Reef of the Bushveld Complex, South Africa. Contrib. Mineral. Petrol. 150, 119–130. https://doi.org/10.1007/s00410-005-0013-z.

Maier, W.D., 2005. Platinum-group element (PGE) deposits and occurrences: Mineralization styles, genetic concepts, and exploration criteria. J. Afr. Earth Sci. 41, 165–191. https://doi.org/10.1016/j.jafrearsci.2005.03.004.

Maier, W.D., de Klerk, L., Blaine, J., Manyeruke, T., Barnes, S.-J., Stevens, M.V.A., Mavrogenes, J.A., 2007. Petrogenesis of contact-style PGE mineralization in the northern lobe of the Bushveld Complex: comparison of data from the farms Rooipoort, Townlands, Drenthe and Nonnenwerth. Mineral. Deposita 43, 255–280. https://doi.org/10.1007/s00126-007-0145-3.

Maier, W.D., Barnes, S.-J., Groves, D.I., 2013. The Bushveld Complex, South Africa : formation of platinum – palladium, chrome- and vanadium-rich layers via hydrodynamic sorting of a mobilized cumulate slurry in a large, relatively slowly cooling, subsiding magma chamber. Mineral. Deposita 48, 1–56. https://doi.org/10.1007/s00126-012-0436-1.

Maier, W.D., Barnes, S.J., Karykowski, B.T., 2016. A chilled margin of komatiite and Mg-rich basaltic andesite in the western Bushveld Complex, South Africa. Contrib. Mineral. Petrol. 171, 1–22. https://doi.org/10.1007/s00410-016-1257-5.

Maier, W.D., Prevec, S.A., Scoates, J.S., Wall, C.J., Barnes, S.J., Gomwe, T., 2017. The Uitkomst intrusion and Nkomati Ni-Cu-Cr-PGE deposit, South Africa: Trace element geochemistry, Nd isotopes and high-precision geochronology. Mineral. Deposita 1–22. https://doi.org/10.1007/s00126-017-0716-x.

Le Maître, R.W., Streckeisen, A., Zanettin, B., Le Bas, M.J., Bonin, B., Bateman, P., Bellieni, G., Dudek, A., Efremova, S., Keller, J., Lameyre, J., Sabine, P.A., Schmid, R., Sorensen, H., Woolley, A.R., 2002. Igneous Rocks. A Classification and Glossary of Terms, Cambridge University Press, Cambridge, United Kingdom. doi:https://doi.org/10.1017/S0016756803388028

Mansur, E.T., 2017. Caracterização e metalogênese do depósito de elementos do grupo da platina do Complexo Luanga, Província Mineral do Carajás. M.Sc. thesis. Universidade de Brasilia.

Mansur, E.T., Ferreira Filho, C.F., 2016. Magmatic structure and geochemistry of the Luanga Mafic–Ultramafic Complex: Further constraints for the PGE-mineralized magmatism in Carajás, Brazil. Lithos, 266–267 28–43. https://doi.org/10.1016/j.lithos.2016.09.036.

Manyeruke, T.D., Maier, W.D., Barnes, S.J., 2005. Major and trace element geochemistry of the Platreef on the farm Townlands, northern Bushveld Complex. South African J. Geol. 108, 381–396. https://doi.org/10.2113/108.3.381.

Martini, J.E.J., Eriksson, P.G., Snyman, C.P., 1995. The early Proterozoic Mississippi Valley-type Pb-Zn-F deposits of the Campbellrand and Malmani Subgroups, South Africa - A review. Miner. Depos. 30, 135–145. https://doi.org/10.1007/BF00189342.

Mavrogenes, J.A., Frost, R., Sparks, H.A., 2013. Experimental evidence of sulphide melt evolution via immiscibility and fractional crystallization. Can. Mineral. 51, 841–850. https://doi.org/10.3749/canmin.51.6.841.

McDonald, I., 2008. Platinum-group element and sulphide mineralogy in ultramafic complexes at western Andriamena, Madagascar. Appl. Earth Sci. IMM Trans. Sect. B 117, 1–10. https://doi.org/10.1179/174327508X309678.

McDonald, I., Holwell, D.A., 2007. Did Lower Zone magma conduits store PGE-rich sulphides that were later supplied to the Platreef? South African J. Geol. 110, 611–616. https://doi.org/10.2113/gssajg.110.4.611.

McDonald, I., Holwell, D.A., Armitage, P.E.B., 2005. Geochemistry and mineralogy of the Platreef and "Critical Zone" of the northern lobe of the Bushveld Complex, South Africa: Implications for Bushveld stratigraphy and the development of PGE mineralisation. Mineral. Deposita 40, 526–549. https://doi.org/10.1007/s00126-005-0018-6.

McDonald, I., Harmer, R.E., Holwell, D.A., Hughes, H.S.R., Boyce, A.J., 2016. Cu-Ni-PGE mineralisation at the Aurora Project and potential for a new PGE province in the Northern Bushveld Main Zone. Ore Geol. Rev. https://doi.org/10.1016/j.oregeorev.2016.09.016.

McSwiggen, P.L., 1999. Platinum-palladium group minerals, gold, silver, and cobalt in the Minamax Copper-Nickel Sulphide Deposit, Duluth Complex, Northeastern Minnesota. Minn. Geol. Surv. Rep., Saint Paul.

Mollo, S., Vona, A., 2014. The geochemical evolution of clinopyroxene in the Roman Province: A window on decarbonation from wall-rocks to magma. Lithos 192, 195, 1–7. https://doi.org/10.1016/j.lithos.2014.01.009.

Mollo, S., Gaeta, M., Freda, C., Di Rocco, T., Misiti, V., Scarlato, P., 2010. Carbonate assimilation in magmas: A reappraisal based on experimental petrology. Lithos 114, 503–514. https://doi.org/10.1016/j.lithos.2009.10.013.

Mudd, G.M., 2012. Key trends in the resource sustainability of platinum group elements. Ore Geol. Rev. 46, 106–117.

Mungall, J.E., 2002. Kinetic controls on the partitioning of trace elements between silicate and sulphide liquids. J. Petrol. 43, 749–768. https://doi.org/10.1093/petrology/43.5.749.

Mungall, J.E., Brenan, J.M., 2003. Experimental evidence for the chalcophile behavior of the halogens. Can. Mineral. 41, 207–220. https://doi.org/10.2113/gscanmin.41.1.207.

Mungall, J.E., Kamo, S.L., McQuade, S., 2016. U–Pb geochronology documents out-of-sequence emplacement of ultramafic layers in the Bushveld Igneous Complex of South Africa. Nat. Commun. 7 (13385), 1–13. https://doi.org/10.1038/ncomms13385.

Murck, B.W., Campbell, I.H., 1986. The effects of temperature, oxygen fugacity and melt composition on the behaviour of chromium in basic and ultrabasic melts. Geochim. Cosmochim. Acta 50, 1871–1887. https://doi.org/10.1016/0016-7037(86)90245-0.

Naldrett, A.J., 2004. Magmatic Sulphide Deposits. Springer-Verlag Berlin Heidelberg New York https://doi.org/10.1180/minmag.1990.054.377.28.

Nell, J., 1985. The Bushveld metamorphic aureole in the Potgietersrus area: evidence for a two-stage metamorphic event. Econ. Geol. 80, 1129–1152. https://doi.org/10.2113/gsecongeo.80.4.1129.

O'Driscoll, B., Donaldson, C.H., Daly, J.S., Emeleus, C.H., 2009. The roles of melt infiltration and cumulate assimilation in the formation of anorthosite and a Cr-spinel seam in the Rum Eastern Layered Intrusion, NW Scotland. Lithos 111, 6–20. https://doi.org/10.1016/j.lithos.2008.11.011.

Oberthür, T., 2011. Platinum-Group Element Mineralization of the Main Sulphide Zone, Great Dyke, Zimbabwe. Rev. Econ. Geol. 17, 329–349.

Paktunc, A.D., Hulbert, L.J., Harris, D.C., 1990. Partitioning of the platinum-group and other trace elements in sulphides from the Bushveld Complex and Canadian occurrences of nicket-copper sulphides. Can. Mineral. 28, 475–488.

Pan Palladium Limited, 2002. December 2002 Quarterly Report.

Pan Palladium Limited, 2008. Notice of General Meeting Explanatory Memorandum (Including the Independent Expert's Report of KPMG Corporate Finance (Aust) Pty Ltd).

Prendergast, M.D., 2012. The Molopo Farms Complex, Southern Botswana - A reconsideration of structure, evolution, and the Bushveld connection. South African J. Geol. 115, 77–90. https://doi.org/10.2113/gssajg.115.1.77.

Prichard, H.M., Knight, R.D., Fisher, P.C., McDonald, I., Zhou, M.F., Wang, C.Y., 2013. Distribution of platinum-group elements in magmatic and altered ores in the Jinchuan intrusion, China: An example of selenium remobilization by postmagmatic fluids. Mineral. Deposita 48, 767–786. https://doi.org/10.1007/s00126-013-0454-7.

Queffurus, M., Barnes, S.J., 2015. A review of sulfur to selenium ratios in magmatic nickel-copper and platinum-group element deposits. Ore Geol. Rev. 69, 301–324. https://doi.org/10.1016/j.oregeorev.2015.02.019.

Reczko, B.F.F., Eriksson, P.G., Snyman, C.P., 1995. Some evidence for the base-metal potential of the Pretoria Group: stratigraphic targets, tectonic setting and REE patterns. Mineral. Deposita 30, 162–167. https://doi.org/10.1007/BF00189345.

Ripley, E.M., Sarkar, A., Li, C., 2005. Mineralogic and stable isotope studies of hydrothermal alteration at the Jinchuan Ni-Cu deposit. China. Econ. Geol. 100, 1349–1361. https://doi.org/10.2113/gsecongeo.100.7.1349.

Roeder, P.L., Reynolds, I., 1991. Crystallization of chromite and chromium solubility in basaltic melts. J. Petrol. 32, 909–934. https://doi.org/10.1093/petrology/32.5.909.

Sasaki, K., Nakashima, K., Kanisawa, S., 2003. Pyrophanite and high Mn ilmenite discovered in the Cretaceous Tono pluton, NE Japan. Neues Jahrb. Mineral. Monatshefte 7, 302–320. https://doi.org/10.1127/0028-3649/2003/2003-0302.

Scandinavian Minerals Limited, 2006. Scandinavian Minerals announces positive drill results from Kevitsa. FinlandNickel-Copper-PGE Property.

Simakin, A.G., Salova, T.P., Bondarenko, G.V., 2012. Experimental study of magmatic melt oxidation by CO_2. Petrology 20, 593–606. https://doi.org/10.1134/S0869591112070053.

Smith, J.W., 2014. The nature and origin of PGE mineralization in the Rooipoort area, northern Bushveld Complex, South Africa. Ph.D. thesis. University of Leicester.

Smith, J.W., Holwell, D.A., McDonald, I., 2014. Precious and base metal geochemistry and mineralogy of the Grasvally Norite–Pyroxenite–Anorthosite (GNPA) member, northern Bushveld Complex, South Africa: implications for a multistage emplacement. Mineral. Deposita 49, 667–692. https://doi.org/10.1007/s00126-014-0515-6.

Smith, J.W., Holwell, D.A., McDonald, I., Boyce, A.J., 2016. The application of S isotopes and S/Se ratios in determining ore-forming processes of magmatic Ni–Cu–PGE sulphide deposits: A cautionary case study from the northern Bushveld Complex. Ore Geol. Rev. 73, 148–174. https://doi.org/10.1016/j.oregeorev.2015.10.022.

Söderholm, K., 2009. Kevitsa Mine - a Big Ni - Cu - PGE Mine in Central Finnish Lapland. Kevitsa Mining/First Quantum Minerals Company Report.

South African Committee for Stratigraphy, 1980. Stratigraphy of South Africa. Republic of South Africa, Dept. of Mineral and Energy Affairs. Geological Survey.

Spandler, C., Mavrogenes, J.A., Arculus, R.J., 2005. Origin of chromitites in layered intrusions: Evidence from chromite-hosted melt inclusions from the Stillwater Complex. Geology 33, 893–896. https://doi.org/10.1130/G21912.1.

Spandler, C., O'Neill, H.S.C., Kamenetsky, V.S., 2007. Survival times of anomalous melt inclusions from element diffusion in olivine and chromite. Nature 447, 303–306. https://doi.org/10.1038/nature05759.

Spandler, C., Martin, L.H.J., Pettke, T., 2012. Carbonate assimilation during magma evolution at Nisyros (Greece), South Aegean Arc: Evidence from clinopyroxenite xenoliths. Lithos 146 (147), 18–33. https://doi.org/10.1016/j.lithos.2012.04.029.

Streckeisen, A., 1976. To each plutonic rock its proper name. Earth Sci. Rev. 12, 1–33. https://doi.org/10.1016/0012-8252(76)90052-0.

Sylvania Resources Ltd, 2010. Sylvania Resources Annonunces Results of Volspruit Metallurgical Testwork and Declaration of JORC Resource.

Tanner, D., Mavrogenes, J.A., Arculus, R.J., Jenner, F.E., 2014. Trace element stratigraphy of the Bellevue Core, Northern Bushveld: Multiple magma injections obscured by diffusive processes. J. Petrol. 55, 859–882. https://doi.org/10.1093/petrology/egu009.

Tao, Y., Li, C., Hu, R., Ripley, E.M., Du, A., Zhong, H., 2007. Petrogenesis of the Pt-Pd mineralized Jinbaoshan ultramafic intrusion in the Permian Emeishan large igneous province, SW China. Contrib. Mineral. Petrol. 153, 321–337. https://doi.org/10.1007/s00410-006-0149-5.

Teigler, B., Eales, H.V., 1996. The Lower and Critical Zones of the Western Limb of the Bushveld Complex as intersected by the Nooitgedacht boreholes. Bull. Geol. Surv. South Africa 111, 1–126.

Teixeira, A.S., Ferreira Filho, C.F., Giustina, M.E.S. Della, Araújo, S.M., da Silva, H.H.A.B., 2015. Geology, petrology and geochronology of the Lago Grande layered complex: Evidence for a PGE-mineralized magmatic suite in the Carajás Mineral Province, Brazil. J. South Am. Earth Sci. 64, 116–138. https://doi.org/10.1016/j.jsames.2015.09.006.

Thakurta, J., Ripley, E.M., Li, C., 2008. Geochemical constraints on the origin of sulphide mineralization in the Duke Island Complex, southeastern Alaska. Geochem. Geophys. Geosyst. 9, 1–34. https://doi.org/10.1029/2008GC001982.

Theart, H.F.J., De Nooy, C.D., 2001. The platinum group minerals in two parts of the massive sulphide body of the Uitkomst Complex, Mpumalanga, South Africa. South African J. Geol. 104, 287–300. doi:https://doi.org/10.2113/104.4.287

Venmyn, 2010. Independent Technical Statement for the Volspruit Project as at 2nd December 2010.

Vukmanovic, Z., Barnes, S.J., Reddy, S.M., Godel, B., Fiorentini, M.L., 2013. Morphology and microstructure of chromite crystals in chromitites from the Merensky Reef (Bushveld Complex, South Africa). Contrib. Mineral. Petrol. 165, 1031–1050. https://doi.org/10.1007/s00410-012-0846-1.

Wang, C.Y., Prichard, H.M., Zhou, M.F., Fisher, P.C., 2008. Platinum-group minerals from the Jinbaoshan Pd-Pt deposit, SW China: Evidence for magmatic origin and hydrothermal alteration. Mineral. Deposita 43, 791–803. https://doi.org/10.1007/s00126-008-0196-0.

Wang, C.Y., Zhou, M.F., Qi, L., 2010. Origin of extremely PGE-rich mafic magma system: An example from the Jinbaoshan ultramafic sill, Emeishan large igneous province, SW China. Lithos 119, 147–161. https://doi.org/10.1016/j.lithos.2010.07.022.

Wenzel, T., Baumgartner, L.P., Konnikov, E.G., Bru, G.E., Kislov, E.V., 2002. Partial melting and assimilation of dolomitic xenoliths by mafic magma: the loko-Dovyren Intrusion (North Baikal Region , Russia). J. Petrol. 43, 2049–2074. https://doi.org/10.1093/petrology/43.11.2049.

Westerlund, K., Gurney, J., Carlson, R., Shirey, S., Hauri, E., Richardson, S., 2004. A metasomatic origin for late Archean eclogitic diamonds: Implications from internal morphology of diamonds and Re-Os and S isotope characteristics of their sulphide inclusions from the late Jurassic Klipspringer kimberlites. South African J. Geol. 107, 119–130.

Wilson, A.H., 2015. The earliest stages of emplacement of the eastern Bushveld Complex: Development of the Lower Zone, Marginal Zone and Basal Ultramafic Sequence. J. Petrol. 56, 347–388. https://doi.org/10.1093/petrology/egv003.

Yang, S.H., Maier, W.D., Hanski, E.J., Lappalainen, M., Santaguida, F., Määttä, S., 2013. Origin of ultra-nickeliferous olivine in the Kevitsa Ni-Cu-PGE-mineralized intrusion, northern Finland. Contrib. Mineral. Petrol. 166, 81–95. https://doi.org/10.1007/s00410-013-0866-5.

Yao, M., Cao, Y., Liu, J., Ren, Z., 2017. Magma mixing as a trigger for sulphide saturation in the UG2 chromitite (Bushveld): Evidence from the silicate and sulphide melt inclusions in chromite. Acta Geol. Sin. - English Ed. 91, 1704–1716.

Yudovskaya, M.A., Kinnaird, J.A., 2010. Chromite in the Platreef (Bushveld Complex, South Africa): Occurrence and evolution of its chemical composition. Mineral. Deposita 45, 369–391. https://doi.org/10.1007/s00126-010-0276-9.

Yudovskaya, M.A., Kinnaird, J.A., Sobolev, A.V., Kuzmin, D.V., McDonald, I., Wilson, A.H., 2013. Petrogenesis of the Lower Zone olivine-rich cumulates beneath the Platreef and their correlation with recognized occurrences in the Bushveld Complex. Econ. Geol. 108, 1923–1952. https://doi.org/10.2113/econgeo.108.8.1923.

Yudovskaya, M.A., Kinnaird, J.A., Udachina, L.V., Distler, V.V., Kuz'min, D.V., 2014. Role of magmatic and fluid concentrating in formation of platinum mineralization in the Lower Zone and Platreef as follows from composition of phlogopite, cumulus silicates, and sulphide melt, the northern limb of Bushveld Complex. Geol. Ore Depos. 56, 451–478. https://doi.org/10.1134/S1075701514060063.

Yudovskaya, M.A., Kinnaird, J.A., Grobler, D.F., Costin, G., Abramova, V.D., Dunnett, T., Barnes, S.-J., 2017. Zonation of Merensky-style platinum-group element mineralization in Turfspruit thick reef facies (northern limb of the Bushveld Complex). Econ. Geol. 112, 1333–1365. https://doi.org/10.5382/econgeo.2017.4512.

Zeh, A., Ovtcharova, M., Wilson, A.H., Schaltegger, U., 2015. The Bushveld Complex was emplaced and cooled in less than one million years - results of zirconology, and geotectonic implications. Earth Planet. Sci. Lett. 418, 103–114. https://doi.org/10.1016/j.epsl.2015.02.035.

Zientek, M.L., Causey, J.D., Parks, H.L., Miller, R.J., 2014. Platinum-group elements in Southern Africa - Mineral inventory and an assessment of undiscovered mineral resources. In: Zientek, M.L., Hammarstrom, J.M., Johnson, K.M. (Eds.), Global Mineral Resource Assessment. United States Geological Survey.